

Frustration and quantum fluctuations in Heisenberg fcc antiferromagnets

T. Yildirim

University of Maryland, College Park, Maryland 20742;

N.I.S.T., Gaithersburg, Maryland 20899;

and Department of Physics, University of Pennsylvania, Philadelphia, Pennsylvania 19104

A. B. Harris

Department of Physics, University of Pennsylvania, Philadelphia, Pennsylvania 19104

and School of Physics and Astronomy, Tel Aviv University, Tel Aviv 69978 Israel

E. F. Shender

Department of Physics, University of California, Berkeley, California 94720

and Institute of Nuclear Physics, St. Petersburg, Russia

(Received 26 November 1997)

We consider the quantum Heisenberg antiferromagnet on a face-centered-cubic lattice in which J , the second-neighbor (intrasublattice) exchange constant, dominates J' , the first-neighbor (intersublattice) exchange constant. It is shown that the continuous degeneracy of the classical ground state with four decoupled (in a mean-field sense) simple cubic antiferromagnetic sublattices is removed so that at second order in J'/J the spins are collinear. Here we study the degeneracy between the two inequivalent collinear structures by analyzing the contribution to the spin-wave zero-point energy which is of the form $\mathcal{H}_{\text{eff}}/J = C_0 + C_4 \sigma_1 \sigma_2 \sigma_3 \sigma_4 (J'/J)^4 + O(J'/J)^5$, where σ_i specifies the phase of the i th collinear sublattice, C_0 depends on J'/J but not on the σ 's, and C_4 is a positive constant. Thus the ground state is one in which the product of the σ 's is -1 . This state, known as the *second kind of type A*, is stable in the range $|J'| < 2|J|$ for large S . Using interacting spin-wave theory, it is shown that the main effect of the zero-point fluctuations is at small wave vector and can be well modeled by an effective biquadratic interaction of the form $\Delta E_Q^{\text{eff}} = -\frac{1}{2} Q \sum_{i,j} [\mathbf{S}(i) \cdot \mathbf{S}(j)]^2 / S^3$. This interaction opens a spin gap by causing the extra classical zero-energy modes to have a nonzero energy of order $J' \sqrt{S}$. We also study the dependence of the zero-point spin reduction on J'/J and the sublattice magnetization on temperature. The resulting experimental consequences are discussed. [S0163-1829(98)01830-X]

I. INTRODUCTION

Interest in quantum fluctuation effects in frustrated magnetic systems has greatly increased in the last few years.¹ The Heisenberg antiferromagnet with nearest-neighbor and next-nearest-neighbor interactions of competing strength is one example of a frustrated quantum spin system.² Another example, one in which the frustration is geometrical (i.e., it does not require adjustment of the magnitude of the coupling constants), is that studied by Shender³ in which spins on a bcc lattice have strong second-neighbor antiferromagnetic interactions and weaker first-neighbor interactions. In that system one therefore has two simple cubic antiferromagnetic sublattices which are decoupled in the mean-field sense. In the classical version of that system the energy is independent of the relative orientations of the two sublattices. In the quantum version of this system, one must consider the selection between classical degenerate ground states which are not equivalent by any symmetry.⁴ Such an analysis, developed in Ref. 3, showed that quantum fluctuations favored a collinear arrangement of sublattices. Based on this result, Henley⁵ proposed that this effect could be described phenomenologically by an effective biquadratic exchange interaction of the form $K[\mathbf{S}_i \cdot \mathbf{S}_j]^2$, where the results of Ref. 3 indicated that K is of order $J'^2/(JS^3)$, where J and J' are coupling constants in-

roduced below. Subsequently many examples of ground-state selection via quantum fluctuations have been analyzed.⁶⁻¹⁰ This phenomenon is the analog of *ordering by disorder* due to thermal fluctuations, a concept discussed by Villain *et al.*¹¹ for Ising systems and then extended to vector spin systems by Henley.^{12,5} The same effect can be realized by configurational fluctuations associated with random substitution in alloys.^{12,13}

In this paper we are concerned with the determination of the ground state of quantum Heisenberg antiferromagnets on a face-centered-cubic (fcc) lattice in the case when the second-neighbor isotropic antiferromagnetic interaction of the form $J\mathbf{S}_i \cdot \mathbf{S}_j$ dominates the isotropic nearest-neighbor interaction (with coupling constant J'), as illustrated in Fig. 1. A seminal study of the classical ground state of this system was given by Yamamoto and Nagamiya.¹⁴ In particular, a relevant structure to study is that which they called type AF-II (we will refer to it as the "second kind"), which has a twofold degeneracy between inequivalent structures called type A and type B, as shown in Fig. 2, and whose domain of stability for the classical ($S \rightarrow \infty$) case is $|J'| < 2|J|$.¹⁵ This degeneracy of the ordering of the second kind was found to be extremely robust: it was not removed by either a tetragonal distortion, or by tetragonal anisotropy.¹⁴ This system may be viewed as four interpenetrating simple cubic antiferro-

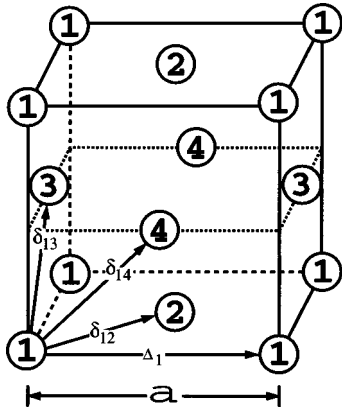


FIG. 1. Four antiferromagnetic sublattices on a fcc lattice. Nearest neighbors within a given simple cubic sublattice are specified by vectors Δ , of which one is shown. Interactions between nearest neighbors on the same sublattice are proportional to J and those between sublattices by J' . A few nearest-neighbor vectors $\delta_{\alpha,\beta}$ connecting different sublattices α and β are also shown. The coordinate axes are chosen such that the x axis is along Δ_1 , the z axis is up, and the y axis is into the page.

magnetic sublattices in which the mean field on one sublattice due to any of the other vanishes. Thus this system provides yet another example of one which classically has a continuous degeneracy which we expect to be lifted by quantum fluctuations.¹ The phenomenological biquadratic interaction mentioned above causes the sublattices to be collinear, but it does not resolve the degeneracy between structures of type A and type B. Recently, we analyzed¹⁰ a similar question for the bct antiferromagnet where collinearity is enforced at relative order $J'^2/(J^2S)$, but to remove the degeneracy associated with different stacking sequences, it was necessary to include the effect of quantum fluctuations to higher order in J'/J . As we shall see, the degeneracy between type A and type B structures is removed when the effects of quantum fluctuations are included to higher order in J'/J . For this type of calculation the formalism introduced

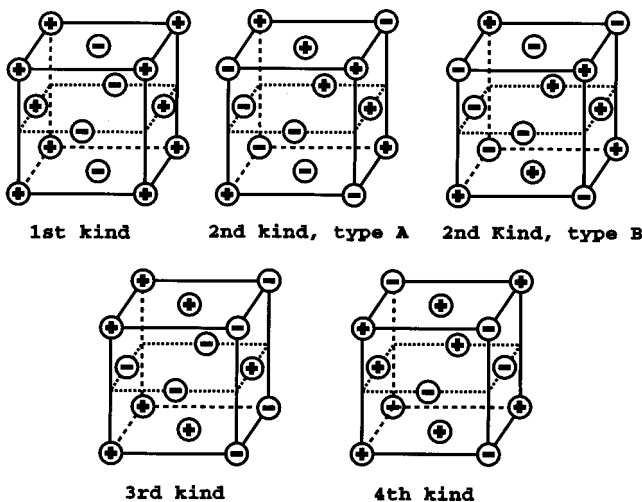


FIG. 2. Various inequivalent collinear spin arrangements in the face-centered cube. (-) and (+) represent spins up and down with respect to any given direction. The coordinate axes are the same as in Fig. 1.

previously¹⁰ is convenient. We also point out that in real systems there may be mechanisms other than quantum fluctuations which could remove the degeneracy between the collinear states. For example, dipolar interactions, single-ion anisotropy, biquadratic exchange interactions, or elastic strain effects due to the dependence of the exchange tensor on atomic displacements, *etc.* may play an important role. However, for the purpose of this paper, we are interested in understanding the effects that quantum fluctuations alone can have on the ground-state selection and therefore we will give little consideration to other possible interactions not included in the isotropic Hamiltonian given below.

A related question in such frustrated systems concerns the nature of the elementary excitations. The Goldstone theorem¹⁶ indicates that at zero wave vector there should be two zero-energy modes. In view of the classical degeneracy associated with the relative rotation of decoupled sublattices, one finds additional zero-energy modes. However, in the presence of quantum fluctuations which remove the classical degeneracy, one can understand the results of Ref. 3, namely that quantum fluctuations cause the extra zero-energy modes to have a nonzero energy at order $J'\sqrt{S}$. Such “quantum gaps” have been observed by inelastic scattering of neutrons.^{17–19} As we shall see, and similar to the results of Ref. 2, in contrast to ground-state selection, the gaps still occur at relative order $J'^2/(J^2S)$ in a calculation of $\omega^2(q)$, even though one must go to higher order in J'/J to completely resolve the structural degeneracy. We calculate the quantum gap at relative order $1/S$ using the Dyson-Maleev²⁰ transformation. This provides an alternative, and possibly simpler, calculation than in Ref. 3.

Briefly this paper is organized as follows. In the next section, we invoke symmetry considerations to write down the most general form of the effective interaction between antiferromagnetic sublattices and then deduce the number of inequivalent collinear spin configurations. In Sec. III we use linearized spin-wave theory to calculate the quantum corrections at first order in $1/S$ due to the zero-point motion. To analyze this complicated expression we follow our previous work¹⁰ and expand the zero-point energy in powers of J'/J to get the effective interaction between sublattices. These interactions lead to the structure experimentally determined for MnO.^{21,22} In Sec. IV we study the spin waves and gaps due to quantum fluctuations by treating spin-wave interactions using the standard Hartree decoupling of the higher-order interaction terms introduced by the Dyson-Maleev transformation²⁰ to bosons. Here we show that the effects of quantum fluctuations can be well approximated (only at zero wave vector) by the effective biquadratic interaction mentioned above. Although a convincing way to demonstrate that an observed gap is caused by quantum fluctuations is to monitor its temperature dependence,^{18,19} we show in an appendix that this conclusion can also be reached by studying how the high-temperature specific heat is related to the observed gap. In Sec. V we study the dependence of the zero-point spin reduction on the ratio J'/J and that of the magnetization on temperature, from which we find that the calculated Néel temperature agrees well with that observed for MnO.^{21,22} Our results are discussed and summarized briefly in Sec. VI.

II. SYMMETRY CONSIDERATIONS

We consider the model

$$\mathcal{H} = \sum_{\langle ij;1 \rangle} J' \mathbf{S}_i \cdot \mathbf{S}_j + \sum_{\langle ij;2 \rangle} J \mathbf{S}_i \cdot \mathbf{S}_j, \quad (1)$$

where $\langle ij;n \rangle$ indicates that the sum is over pairs of n th nearest neighbors. We are mainly concerned with the case when J is dominant, and the system can be considered to be four interpenetrating simple cubic antiferromagnetic sublattices. As we mentioned previously, the effect of quantum fluctuations at second order in J'/J is to cause the spins to be arranged collinearly.³ Therefore, for the α th simple cubic antiferromagnetic sublattice we introduce an Ising variable σ_α to specify its phase, so that σ_α gives the value of S_z for the spin at position τ_α , where τ_α is given in Table I. In terms of these variables, the ground-state energy, i.e., the effective interaction, denoted \mathcal{H}_{eff} , then must be of the form:

$$\mathcal{H}_{\text{eff}}/J = C_0 + C_2(\sigma_1\sigma_2 + \dots + \sigma_3\sigma_4) + C_4\sigma_1\sigma_2\sigma_3\sigma_4, \quad (2)$$

where the coefficients C_n depend on J'/J and $1/S$. In writing this result we omitted odd-order terms in the σ_i , since the original Hamiltonian of Eq. (1) is invariant under $\mathbf{S}_i \rightarrow -\mathbf{S}_i$ for all i . Now it is possible to eliminate some terms in Eq. (2) using the symmetry operations of the system. First of all, the reflection operation with respect to the $[100]$, $[010]$, or $[001]$ planes should not change the energy. Since these symmetry operations change the sign of any two σ_i , the coefficients C_2 in Eq. (2) must be zero. Thus we have

$$\mathcal{H}_{\text{eff}}/J = C_0 + C_4\sigma_1\sigma_2\sigma_3\sigma_4. \quad (3)$$

Since there is no symmetry operation which changes the sign of the only one σ_i (or equivalently, three of them), the term $\sigma_1\sigma_2\sigma_3\sigma_4$ is allowed by symmetry. It therefore follows that we have two inequivalent collinear spin arrangement in which $\sigma_1\sigma_2\sigma_3\sigma_4$ is minus or plus one. (See Fig. 2.) The first one where $\sigma_1\sigma_2\sigma_3\sigma_4 = -1$ is called ‘‘the second kind of type A.’’ For this configuration it is possible to find a unique $[111]$ direction, perpendicular to which, each net plane contains a ferromagnetic array of spins and the sequence of such net planes is stacked antiferromagnetically. In other words, this structure has trigonal crystal symmetry and is therefore subject to a rhombohedral distortion. In contrast, ordering of ‘‘the second kind of type B’’ (also shown in Fig. 2) for which $(\sigma_1\sigma_2\sigma_3\sigma_4 = 1)$, still has cubic symmetry. In order to determine which of these structures is really the ground-state configuration, we therefore need to know the sign of C_4 in Eq. (3). In the next section we shall calculate

TABLE I. Origins of the four sublattices, τ_α , used in the calculations.

Sublattice, α	$\tau_\alpha = (x_\alpha, y_\alpha, z_\alpha)$
1	(0,0,0)
2	$\frac{1}{2}(a, a, 0)$
3	$\frac{1}{2}(0, a, a)$
4	$\frac{1}{2}(a, 0, a)$

C_4 by linear spin-wave theory and show that the leading contribution is a positive one of order $(J'/J)^4 S^{-1}$.

III. LINEARIZED SPIN-WAVE THEORY

To obtain the sign of C_4 we recall that $C_4 = 0$ for $S = \infty$. This result shows the degeneracy for the classical case analyzed by Yamamoto and Nagamiya.¹⁴ Therefore, we work to relative order $1/S$, which involves calculating the quantum zero-point energy of spin waves. At this order in $1/S$, for this energy to be a function of four σ 's, we must involve four J' 's. (To see this recall that zero-point fluctuations involve creating a pair of spin excitations on different sublattices. In this picture, a contribution to the ground-state energy which involves all four sublattices requires creating two pairs of spin excitations to cover the four sublattices and then subsequently destroying two pairs of excitations.) As we shall see, we obtain a nonzero result for C_4 at order $(J'/J)^4/S$. So going to higher order in $1/S$ cannot lead to a result lower order in (J'/J) .

As mentioned, when J' is sufficiently small, the system forms four simple cubic antiferromagnetic sublattices. We therefore write the Hamiltonian of Eq. (1) as

$$\mathcal{H} = J \sum_{\langle \alpha i, \alpha j; 2 \rangle} \mathbf{S}_\alpha(i) \mathbf{S}_\alpha(j) + J' \sum_{\langle \alpha i, \beta j; 1 \rangle} \mathbf{S}_\alpha(i) \mathbf{S}_\beta(j), \quad (4)$$

where $S_\alpha(i)$ denotes the i th spin on sublattice α . The first term on the right-hand side of Eq. (4) is the interaction within the sublattices and second term is that between sublattices.

Within the classical approximation the four sublattices may assume arbitrary relative orientations in the ground state. It is known that in such a situation quantum fluctuations select collinear structures.^{3,23,24} We could verify this result here by evaluating the zero-point energy when the four sublattices are arbitrarily oriented. However, in the interest of simplicity, we will assume that the spin structure is collinear, so that all spins lie along the positive or negative z axis and the magnetic structure is characterized by a wave vector \mathbf{Q} and a phase θ_α such that the phase of S_z at site i in sublattice α ,

$$\phi_\alpha(i) = \mathbf{Q} \cdot \mathbf{r}_i + \theta_\alpha, \quad (5)$$

TABLE II. Wave vectors \mathbf{Q} and phases θ_α of Eq. (5) for the structures shown in Fig. 2. Since each component of \mathbf{Q} is an integer multiple of π/a (where a is defined in Fig. 1), we may restrict each component to assume the values 0 or π/a . Application of elements of cubic symmetry lead to structures equivalent to those shown. E.g., taking $\mathbf{Q} = (0, \pi/a, 0)$ leads to a structure equivalent to that of the third kind shown in Fig. 2.

Kind (type) of structure	$a\mathbf{Q}$	$\{\theta_\alpha\}$
1	(0,0,0)	(0, π , 0, π)
2A	(π , π , π)	(0,0,0,0)
2B	(π , π , π)	(0, π , 0, 0)
3	(π , 0, 0)	(0, $-\pi/2$, π , $\pi/2$)
4	(π , π , 0)	(0, π , $-\pi/2$, $\pi/2$)

is a multiple of π . For the spin-wave expansion we introduce local axes at site i in sublattice α , so that the S'_z axis lies along the direction in which the spin points in the ground state:

$$\mathbf{S}_\alpha(i) = \begin{pmatrix} 1 & 0 & 0 \\ 0 & \cos(\mathbf{Q} \cdot \mathbf{r}_i + \theta_\alpha) & 0 \\ 0 & 0 & \cos(\mathbf{Q} \cdot \mathbf{r}_i + \theta_\alpha) \end{pmatrix} \mathbf{S}'_\alpha(i), \quad (6)$$

where, using Dyson-Maleev transformation, we have

$$S'_x(i) = \sqrt{\frac{S}{2}} \left[a_\alpha^+(i) + a_\alpha(i) - \frac{1}{2S} a_\alpha^+(i) a_\alpha^+(i) a_\alpha(i) \right], \quad (7)$$

$$S'_y(i) = i \sqrt{\frac{S}{2}} \left[a_\alpha^+(i) - a_\alpha(i) - \frac{1}{2S} a_\alpha^+(i) a_\alpha^+(i) a_\alpha(i) \right], \quad (8)$$

$$S'_z(i) = S - a_\alpha^+(i) a_\alpha(i). \quad (9)$$

All the structures shown in Fig. 2 are described by a single wave vector (but with appropriate choice of θ_α for each sublattice), as listed in Table II. In particular, for the structures of the second kind, one has

$$\mathbf{Q} = (\pi/a, \pi/a, \pi/a), \quad (10)$$

where a is defined in Fig. 1.

From Eq. (6) one can write

$$\mathbf{S}_\alpha(i) \cdot \mathbf{S}_\beta(j) = S^2 \cos(\theta_{j\beta, i\alpha}) + \hat{O}_{j\beta, i\alpha}^{(2)} + \hat{O}_{j\beta, i\alpha}^{(4)} + O(1/S), \quad (11)$$

where the quadratic term is

$$\begin{aligned} \hat{O}_{j\beta, i\alpha}^{(2)} = & -S \cos(\theta_{j\beta, i\alpha}) [a_\alpha^+(i) a_\alpha(i) + a_\beta^+(j) a_\beta(j)] + \frac{1}{2} S [1 + \cos(\theta_{j\beta, i\alpha})] [a_\alpha^+(i) a_\beta(j) + a_\alpha(i) a_\beta^+(j)] \\ & + \frac{1}{2} S [1 - \cos(\theta_{j\beta, i\alpha})] [a_\alpha^+(i) a_\beta^+(j) + a_\alpha(i) a_\beta(j)], \end{aligned} \quad (12)$$

where

$$\theta_{j\beta, i\alpha} = \mathbf{Q} \cdot (\mathbf{r}_j - \mathbf{r}_i) + \theta_\beta - \theta_\alpha \quad (13)$$

is the angle between spin i in sublattice α and spin j in sublattice β . In Eq. (11) $\hat{O}_{j\beta, i\alpha}^{(4)}$ is the four-operator term which is discussed in Sec. IV B.

For the structures of the second kind (see Fig. 2), we use Eq. (12) to write the Hamiltonian up to terms quadratic in the boson operators as

$$\mathcal{H} = E_0 + \mathcal{H}_0 + \mathcal{H}_I, \quad (14)$$

where

$$E_0 = -12NJS^2 [1 + (1/S)], \quad (15)$$

$$\mathcal{H}_0 = 3JS \sum_{\alpha, \mathbf{q}} \{ a_\alpha^+(\mathbf{q}) a_\alpha(\mathbf{q}) + a_\alpha(\mathbf{q}) a_\alpha^+(\mathbf{q}) + \gamma(\mathbf{q}) [a_\alpha^+(\mathbf{q}) a_\alpha^+(-\mathbf{q}) + a_\alpha(\mathbf{q}) a_\alpha(-\mathbf{q})] \}, \quad (16)$$

where

$$\begin{aligned} \gamma(\mathbf{q}) &= \frac{1}{6} \sum_{\Delta} e^{i\mathbf{q} \cdot \Delta} \\ &= (1/3) [\cos(q_x a) + \cos(q_y a) + \cos(q_z a)], \end{aligned} \quad (17)$$

and \mathcal{H}_I is the interaction between sublattices. Also N is the number of the sites in each of the four simple cubic antiferromagnetic sublattice, \mathbf{q} is summed over N values in the interval $-\pi < aq_\alpha < \pi$ ($\alpha = x, y, z$), and we introduced Fourier transformed variables by

$$a_\alpha^+(i) = \frac{1}{\sqrt{N}} \sum_{\mathbf{q}} a_\alpha^+(\mathbf{q}) e^{i\mathbf{q} \cdot \mathbf{r}_i}. \quad (18)$$

Thus this representation is based on a reciprocal lattice with basis vectors

$$\begin{aligned} \mathbf{b}_1 &= (2\pi/a)(1, 0, 0), & \mathbf{b}_2 &= (2\pi/a)(0, 1, 0), \\ \mathbf{b}_3 &= (2\pi/a)(0, 0, 1), \end{aligned} \quad (19)$$

whose unit cell we will refer to as the simple cubic (sc) Brillouin zone (BZ). Note that \mathcal{H}_0 represents the sum of independent Hamiltonians for each of the antiferromagnetic sublattices, which, in the absence of \mathcal{H}_I , are completely decoupled.

It is useful to compare this formulation for four interpenetrating antiferromagnetic subsystems with that for a single antiferromagnetic system on a simple cubic lattice. In the

usual (two sublattice) formulation of an antiferromagnet, one introduces operators $a^+(i)$ and $b^+(j)$ which create excitations on the a (up) and b (down) sublattices. Then the magnetic unit cell contains two spins and the corresponding magnetic BZ is half as large as the sc BZ. In this two sublattice picture each mode is doubly degenerate. This doubly degenerate spectrum can be obtained by ‘‘folding over’’ the single mode spectrum of the sc BZ, because for the sc BZ spectrum the modes at \mathbf{q} and $\mathbf{q}+(\pi/a)(1,1,1)$ are degenerate. [One can see this from Eq. (37), below, noting that for both these wave vectors $\gamma(\mathbf{q})^2$ is the same.] Applied to the present case of four antiferromagnetic subsystems, the situation is as follows. In the representation based on a sc BZ and in the absence of interactions between subsystems, each of the mode of the antiferromagnet is fourfold degenerate. When \mathcal{H}_I is taken into account, one obtains four modes which are nondegenerate at a generic point in phase space. However, because the mean field at one sublattice due to another one vanishes, within linearized spin-wave theory, even when \mathcal{H}_I is included, all four modes will have vanishing energy as the reduced wave vector goes to zero. Counting both the modes at $\mathbf{q}=0$ and those at $\mathbf{q}=(\pi/a)(1,1,1)$, we see that within linearized spin-wave theory there are then eight Goldstone modes. As we will see later, interactions give six of these modes a nonzero energy, so that, as expected, we are left with only two true Goldstone modes.

The interaction between sublattices is

$$H_I = J'S \sum_{\alpha,\beta,\mathbf{q}} \{A_{\alpha\beta}(\mathbf{q})[a_{\alpha}^+(\mathbf{q})a_{\beta}(\mathbf{q}) + a_{\alpha}(\mathbf{q})a_{\beta}^+(\mathbf{q})] + B_{\alpha\beta}(\mathbf{q})[a_{\alpha}^+(\mathbf{q})a_{\beta}^+(-\mathbf{q}) + a_{\alpha}(\mathbf{q})a_{\beta}(-\mathbf{q})]\}, \quad (20)$$

where $A_{\alpha\alpha}=B_{\alpha\alpha}=0$, and, for $\alpha \neq \beta$, we have

$$A_{\alpha\beta}(\mathbf{q}) = \frac{1}{4} \sum_{\vec{\delta}_{\alpha,\beta}} [1 + \cos(\mathbf{Q} \cdot \vec{\delta}_{\alpha,\beta} + \theta_{\beta} - \theta_{\alpha})] e^{-i\mathbf{q} \cdot \vec{\delta}_{\alpha,\beta}}, \quad (21a)$$

$$B_{\alpha\beta}(\mathbf{q}) = \frac{1}{4} \sum_{\vec{\delta}_{\alpha,\beta}} [1 - \cos(\mathbf{Q} \cdot \vec{\delta}_{\alpha,\beta} + \theta_{\beta} - \theta_{\alpha})] e^{-i\mathbf{q} \cdot \vec{\delta}_{\alpha,\beta}}, \quad (21b)$$

where $\vec{\delta}_{\alpha,\beta}$ is summed over the four first-neighbor vectors which connect sublattices α and β , as shown in Fig. 1.

We now specialize to structures of the second kind, with \mathbf{Q} given by Eq. (10). For such collinear structures we may characterize the orientation of sublattice α by an Ising variable σ_{α} which specifies the sign of S_z at the origin, τ_{α} , of α sublattice. Inserting the values of τ_{α} from Table I, we see that Eq. (5) gives

$$\cos \theta_{\alpha} = \begin{cases} \sigma_{\alpha} & \text{if } \alpha = 1 \\ -\sigma_{\alpha} & \text{otherwise.} \end{cases} \quad (22)$$

Equation (21) can be rewritten as

$$A_{\alpha\beta}(\mathbf{q}) = C_{\alpha\beta}(\mathbf{q}) + S_{\alpha\beta}(\mathbf{q}), \quad (23a)$$

$$B_{\alpha\beta}(\mathbf{q}) = C_{\alpha\beta}(\mathbf{q}) - S_{\alpha\beta}(\mathbf{q}), \quad (23b)$$

where $C_{\alpha\beta}(\mathbf{q})$ and $S_{\alpha\beta}(\mathbf{q})$ are the matrix elements of the matrices

$$\mathbf{C}(\mathbf{q}) = \begin{bmatrix} 0 & c_{xy}(\mathbf{q}) & c_{yz}(\mathbf{q}) & c_{xz}(\mathbf{q}) \\ c_{xy}(\mathbf{q}) & 0 & c_{xz}(\mathbf{q}) & c_{yz}(\mathbf{q}) \\ c_{yz}(\mathbf{q}) & c_{xz}(\mathbf{q}) & 0 & c_{xy}(\mathbf{q}) \\ c_{xz}(\mathbf{q}) & c_{yz}(\mathbf{q}) & c_{xy}(\mathbf{q}) & 0 \end{bmatrix} \quad (24)$$

and

$$\mathbf{S}(\mathbf{q}) = \begin{bmatrix} 0 & -\sigma_1\sigma_2s_{xy}(\mathbf{q}) & -\sigma_1\sigma_3s_{yz}(\mathbf{q}) & -\sigma_1\sigma_4s_{xz}(\mathbf{q}) \\ -\sigma_2\sigma_1s_{xy}(\mathbf{q}) & 0 & \sigma_2\sigma_3s_{xz}(\mathbf{q}) & \sigma_2\sigma_4s_{yz}(\mathbf{q}) \\ -\sigma_3\sigma_1s_{yz}(\mathbf{q}) & \sigma_3\sigma_2s_{xz}(\mathbf{q}) & 0 & \sigma_3\sigma_4s_{xy}(\mathbf{q}) \\ -\sigma_4\sigma_1s_{xz}(\mathbf{q}) & \sigma_4\sigma_2s_{yz}(\mathbf{q}) & \sigma_4\sigma_3s_{xy}(\mathbf{q}) & 0 \end{bmatrix}, \quad (25)$$

where $s_{\mu\nu}(\mathbf{q})$ and $c_{\mu\nu}(\mathbf{q})$ ($\mu, \nu = x, y, \text{ or } z$) are

$$s_{\mu\nu}(\mathbf{q}) = \sin(q_{\mu}a/2) \sin(q_{\nu}a/2), \quad (26)$$

$$c_{\mu\nu}(\mathbf{q}) = \cos(q_{\mu}a/2) \cos(q_{\nu}a/2).$$

The bilinear Hamiltonian in Eq. (14) can be written in matrix form as

$$\mathcal{H} = E_0 + \frac{1}{2} \sum_{\mathbf{q}} \mathbf{X}^+(\mathbf{q}) \mathbf{M}(\mathbf{q}) \mathbf{X}(\mathbf{q}). \quad (27)$$

Here

$$\mathbf{X}(\mathbf{q}) = \begin{pmatrix} \mathbf{V}(\mathbf{q}) \\ \mathbf{V}^+(-\mathbf{q}) \end{pmatrix}, \quad (28)$$

with

$$\mathbf{V}(\mathbf{q}) = \begin{pmatrix} a_1(\mathbf{q}) \\ a_2(\mathbf{q}) \\ a_3(\mathbf{q}) \\ a_4(\mathbf{q}) \end{pmatrix} \quad (29)$$

and the matrix $\mathbf{M}(\mathbf{q})$ is

$$\mathbf{M}(\mathbf{q}) = \begin{pmatrix} \mathbf{H}_1(\mathbf{q}) & \mathbf{H}_2(\mathbf{q}) \\ \mathbf{H}_2(\mathbf{q}) & \mathbf{H}_1(\mathbf{q}) \end{pmatrix}, \quad (30)$$

where \mathbf{H}_1 and \mathbf{H}_2 are the four-dimensional matrices

$$\mathbf{H}_1(\mathbf{q}) = 6JS\{\mathbf{I} + [J'/(3J)]\mathbf{A}(\mathbf{q})\}, \quad (31a)$$

$$\mathbf{H}_2(\mathbf{q}) = 6JS\{\gamma(\mathbf{q})\mathbf{I} + [J'/(3J)]\mathbf{B}(\mathbf{q})\}. \quad (31b)$$

Here \mathbf{I} is the four-dimensional unit matrix and the matrix elements of $\mathbf{A}(\mathbf{q})$ and $\mathbf{B}(\mathbf{q})$ were given in Eqs. (21). After diagonalizing the matrix $\mathbf{M}(\mathbf{q})$, one finds that the Hamiltonian in Eq. (27) can be written in terms of normal mode operators $c_\alpha^+(\mathbf{q})$ and $c_\alpha(\mathbf{q})$ as

$$\mathcal{H} = E_0 + \Delta E_Q + \sum_{\alpha, \mathbf{q}} \omega_\alpha(\mathbf{q}) c_\alpha^+(\mathbf{q}) c_\alpha(\mathbf{q}), \quad (32)$$

where $\alpha = 1, 2, 3, 4$ labels the eigenvalues of $\mathbf{M}(\mathbf{q})$ and where the first quantum correction, ΔE_Q , is

$$\Delta E_Q = \frac{1}{2} \sum_{\alpha, \mathbf{q}} \omega_\alpha(\mathbf{q}). \quad (33)$$

Here the $\omega_\alpha(\mathbf{q})$ are the positive square roots of the roots of the characteristic equation of the dynamical matrix $\mathbf{D}(\mathbf{q})$

$$\mathbf{D}(\mathbf{q}) = [\mathbf{H}_1(\mathbf{q}) + \mathbf{H}_2(\mathbf{q})][\mathbf{H}_1(\mathbf{q}) - \mathbf{H}_2(\mathbf{q})] \quad (34)$$

$$= E_0^2(\mathbf{q})[\mathbf{I} + 4j\mathbf{P}(\mathbf{q})][\mathbf{I} + 4j\mathbf{R}(\mathbf{q})], \quad (35)$$

where

$$j = J'/(6J), \quad (36)$$

$$E_0(\mathbf{q}) = 6JS\sqrt{1 - \gamma^2(\mathbf{q})}, \quad (37)$$

and the matrices \mathbf{P} and \mathbf{R} are

$$\mathbf{P}(\mathbf{q}) = \frac{1}{2[1 + \gamma(\mathbf{q})]} [\mathbf{A}(\mathbf{q}) + \mathbf{B}(\mathbf{q})] = \frac{1}{1 + \gamma(\mathbf{q})} \mathbf{C}(\mathbf{q}), \quad (38)$$

$$\mathbf{R}(\mathbf{q}) = \frac{1}{2[1 - \gamma(\mathbf{q})]} [\mathbf{A}(\mathbf{q}) - \mathbf{B}(\mathbf{q})] = \frac{1}{1 - \gamma(\mathbf{q})} \mathbf{S}(\mathbf{q}). \quad (39)$$

We may use Eq. (33) to express the zero-point energy per site in dimensionless units, $\Delta E'_Q$, as

$$\begin{aligned} \Delta E'_Q &\equiv \Delta E_Q / (12NJS^2) = \frac{1}{24NJS^2} \sum_{\mathbf{q}} \text{tr}(\sqrt{\mathbf{D}}) \\ &= \frac{1}{24NJS^2} \sum_{\mathbf{q}} E_0(\mathbf{q}) \text{tr}(\sqrt{\mathbf{I} + \mathbf{Y}_q}) \equiv \frac{1}{4S} \langle \text{tr}(\sqrt{\mathbf{I} + \mathbf{Y}_q}) \rangle_{\mathbf{q}} \\ &\equiv \frac{1}{S} \Delta e_Q, \end{aligned} \quad (40)$$

so that $S^{-1}\Delta e_Q$ is the correction to the ground-state energy in dimensionless units at relative order $1/S$, and

$$\mathbf{Y}_q = 4j[P(\mathbf{q}) + R(\mathbf{q})] + 16j^2P(\mathbf{q})R(\mathbf{q}) \quad (41)$$

and $\langle \dots \rangle_{\mathbf{q}}$ represents the following \mathbf{q} summation over the first Brillouin zone:

$$\begin{aligned} \langle f(\mathbf{q}) \rangle_{\mathbf{q}} &= \frac{1}{6NJS} \sum_{\mathbf{q}} E_0(\mathbf{q}) f(\mathbf{q}) \\ &= \left(\frac{a}{2\pi}\right)^3 \int_{-\pi/a}^{\pi/a} dq_x \int_{-\pi/a}^{\pi/a} dq_y \\ &\quad \times \int_{-\pi/a}^{\pi/a} dq_z \sqrt{1 - \gamma(\mathbf{q})^2} f(\mathbf{q}). \end{aligned} \quad (42)$$

To get an analytical expression for the effective interaction between antiferromagnetic sublattices, we now follow Ref. 10 and expand Δe_Q in powers of j . For the regime of interest $|J'| < 2|J|$, $j = [J'/(6J)] < 1/3$. Therefore we write Δe_Q in Eq. (40) as

$$\Delta e_Q = \sum_{n=0}^{\infty} C_n \langle \text{tr}(\mathbf{Y}_q^n) \rangle_{\mathbf{q}},$$

$$C_n = (-1)^{n-1} \frac{(2n)!}{2^{2n+2}(n!)^2(2n-1)}, \quad (43)$$

and then collect the terms which are of the same order in j to get Δe_Q in the form

$$\begin{aligned} \Delta e_Q &= \Delta e_Q^{(0)} + \Delta e_Q^{(2)}j^2 + \Delta e_Q^{(3)}j^3 + \Delta e_Q^{(4)}j^4 \\ &\quad + \Delta e_Q^{(5)}j^5 + O(j^6). \end{aligned} \quad (44)$$

In above expansion we have two types of terms. The first one is a term like $\langle \text{tr}(\mathbf{P}^m \mathbf{R}^n) \rangle_{\mathbf{q}}$. This type of term cannot depend on Ising variables $\sigma_\alpha \sigma_\beta$ because of the form of the matrix \mathbf{R} . [See Eqs. (39) and (25).] We can see this easily by realizing that the matrix \mathbf{R}^n (where n is a positive integer) has the same form as \mathbf{R} : namely, its nonzero diagonal elements do not depend on σ_α because $\sigma_\alpha^2 = 1$. The off-diagonal entry, $[\mathbf{R}^n]_{\alpha\beta}$ is proportional to $\sigma_\alpha \sigma_\beta \sin(q_\mu a/2) \sin(q_\nu a/2)$ times a function which is even in q_x , q_y , and q_z . Note also that all matrix elements of \mathbf{P} are even functions of momenta. Therefore all terms in $\langle \text{tr}(\mathbf{P}^m \mathbf{R}^n) \rangle_{\mathbf{q}}$ which depend on the σ_α 's vanish when the sum over \mathbf{q} is performed. The second type of terms are those of the form $\langle \text{tr}(\mathbf{P}^{l_1} \mathbf{R}^{l_2} \mathbf{P}^{l_3} \mathbf{R}^{l_4} \dots \mathbf{P}^{l_k}) \rangle_{\mathbf{q}}$ with l_1, l_2, \dots nonzero. Such terms can depend on σ_α . From Eqs. (41) and (43) we see that the term $\langle \text{tr}(\mathbf{P}\mathbf{R}\mathbf{P}\mathbf{R}) \rangle_{\mathbf{q}}$ first occurs at fourth order in J'/J , so that

$$\begin{aligned} \Delta e_Q &= \text{const} + 256[C_2 + 3C_3 + 2C_4] \langle \text{tr}(\mathbf{P}\mathbf{R}\mathbf{P}\mathbf{R}) \rangle_{\mathbf{q}} j^4 \\ &= \text{const} - \langle \text{tr}(\mathbf{P}\mathbf{R}\mathbf{P}\mathbf{R}) \rangle_{\mathbf{q}} j^4, \end{aligned} \quad (45)$$

where const denotes terms which are independent of the σ_α 's. After a little algebra one finds that

$$\begin{aligned} \Delta e_Q &= \text{const} + 4 \langle \hat{C}_{xz}^2 (\hat{S}_{xy}^2 + \hat{S}_{yz}^2) + \hat{C}_{xy}^2 (\hat{S}_{xz}^2 + \hat{S}_{yz}^2) \\ &\quad + \hat{C}_{yz}^2 (\hat{S}_{xz}^2 + \hat{S}_{xy}^2) \rangle_{\mathbf{q}} \sigma_1 \sigma_2 \sigma_3 \sigma_4 j^4 \\ &= \text{const} + 24 \langle \hat{C}_{xz}^2 \hat{S}_{xy}^2 \rangle_{\mathbf{q}} \sigma_1 \sigma_2 \sigma_3 \sigma_4 j^4, \end{aligned} \quad (46)$$

where

$$\hat{S}_{\mu\nu} = \frac{1}{1 - \gamma(\mathbf{q})} \sin\left(\frac{q_\mu a}{2}\right) \sin\left(\frac{q_\nu a}{2}\right) \quad \mu, \nu = x, y, z \quad (47)$$

$$\hat{C}_{\mu,\nu} = \frac{1}{1 + \gamma(\mathbf{q})} \cos\left(\frac{q_\mu a}{2}\right) \cos\left(\frac{q_\nu a}{2}\right) \quad \mu, \nu = x, y, z. \quad (48)$$

From this equation, we see that zero-point fluctuations select the collinear spin arrangement where $\sigma_1\sigma_2\sigma_3\sigma_4 = -1$ as the ground state. This type spin arrangement is called *the second kind of type A* by Yamamoto and Nagamiya.¹⁴ They call the other collinear arrangement in which the product $\sigma_1\sigma_2\sigma_3\sigma_4 = 1$ *the second kind of type B*. The difference in energy between these two collinear configurations is

$$\begin{aligned} \Delta e_Q^A - \Delta e_Q^B &= -8\langle \hat{C}_{xz}^2 (\hat{S}_{xy}^2 + \hat{S}_{yz}^2) + \hat{C}_{xy}^2 (\hat{S}_{xz}^2 + \hat{S}_{yz}^2) \\ &\quad + \hat{C}_{yz}^2 (\hat{S}_{xz}^2 + \hat{S}_{xy}^2) \rangle_q j^4 \\ &= -1.8069j^4 \\ &= -1.3942 \times 10^{-3} \text{ for } J' = J. \end{aligned} \quad (49)$$

Using the algebraic computational computer program MATHEMATICA, one can easily get the following expressions for the terms $\Delta e_Q^{(n)}$ ($n = 1, 2, \dots$) in Eq. (44):

$$\Delta e_Q^{(0)} = \langle 1 \rangle_q, \quad (50)$$

$$\Delta e_Q^{(2)} = -12 \langle \hat{S}_{xy}^2 \rangle_q, \quad (51)$$

$$\Delta e_Q^{(3)} = 48 \langle \hat{S}_{xy} \hat{S}_{yz} \hat{S}_{zx} \rangle_q, \quad (52)$$

$$\begin{aligned} \Delta e_Q^{(4)} &= 24 \langle \hat{S}_{xy}^2 \hat{C}_{xz}^2 \rangle_q \sigma_1 \sigma_2 \sigma_3 \sigma_4 - 60 \langle \hat{S}_{xy}^4 \rangle_q - 360 \langle \hat{S}_{xy}^2 \hat{S}_{xz}^2 \rangle_q \\ &\quad + 48 \langle \hat{S}_{xy}^2 \hat{C}_{xz}^2 \rangle_q + 12 \langle \hat{S}_{xy}^2 \hat{C}_{xy}^2 \rangle_q, \end{aligned} \quad (53)$$

$$\begin{aligned} \Delta e_Q^{(5)} &= -288 \langle \hat{S}_{xy} \hat{S}_{yz} \hat{S}_{zx} \hat{C}_{xy}^2 \rangle_q \sigma_1 \sigma_2 \sigma_3 \sigma_4 \\ &\quad + 3360 \langle \hat{S}_{xy} \hat{S}_{yz} \hat{S}_{zx} \hat{S}_{xy}^2 \rangle_q - 576 \langle \hat{S}_{xy} \hat{S}_{yz} \hat{S}_{zx} \hat{C}_{xy}^2 \rangle_q. \end{aligned} \quad (54)$$

In writing the above expressions, we used the fact that from symmetry $\langle \hat{S}_{\mu\nu}^2 \rangle_q = \langle \hat{C}_{\mu\nu}^2 \rangle_q$ and other similar equalities obtained with different permutations of $\mu, \nu = x, y, z$. After integrating these expressions numerically, results from which are listed in Table III, the zero-point energy given in Eq. (44) is obtained as

$$\begin{aligned} \Delta e_Q &= \Delta E_Q / (12NJS) \\ &= 0.90285 - 2.0484j^2 + 2.3031j^3 \\ &\quad + (0.90345\sigma_1\sigma_2\sigma_3\sigma_4 - 9.98298)j^4 \\ &\quad - (2.63993\sigma_1\sigma_2\sigma_3\sigma_4 - 41.1674)j^5. \end{aligned} \quad (55)$$

In order to corroborate our analytical work, we have also diagonalized the matrix numerically and then calculated the zero-point energy from Eq. (33) for different spin configurations. For instance, Fig. 3 shows the zero-point energy per spin for $J' = J$ as a function of spin orientation of four sub-

TABLE III. Numerical values of the expressions obtained in Eqs. (50)–(53). Here $\langle f(\mathbf{q}) \rangle_q = (a/2\pi)^3 \int_{-\pi/a}^{\pi/a} \int_{-\pi/a}^{\pi/a} \int_{-\pi/a}^{\pi/a} d^3\mathbf{q} \sqrt{1 - \gamma(\mathbf{q})^2} f(\mathbf{q})$.

$\langle f(\mathbf{q}) \rangle_q$	Numerical value
$\langle 1 \rangle_q$	9.0284×10^{-1}
$\langle \hat{S}_{xy}^2 \rangle_q$	1.7070×10^{-1}
$\langle \hat{S}_{xy}^4 \rangle_q$	5.6635×10^{-2}
$\langle \hat{S}_{xy}^2 \hat{C}_{xy}^2 \rangle_q$	2.0281×10^{-2}
$\langle \hat{S}_{xy}^2 \hat{C}_{xz}^2 \rangle_q$	3.7644×10^{-2}
$\langle \hat{S}_{xy}^2 \hat{S}_{xz}^2 \rangle_q$	2.3987×10^{-2}
$\langle \hat{S}_{xy} \hat{S}_{yz} \hat{S}_{zx} \rangle_q$	4.7980×10^{-2}
$\langle \hat{S}_{xy} \hat{S}_{yz} \hat{S}_{zx} \hat{C}_{xy}^2 \rangle_q$	1.0681×10^{-2}
$\langle \hat{S}_{xy} \hat{S}_{yz} \hat{S}_{zx} \hat{C}_{xy}^2 \rangle_q$	0.9166×10^{-2}

lattices. Collinear spin configurations denoted by A and E at the right side of the figure have much lower energy than noncollinear configurations. The energy difference between two nonequivalent collinear states A ($\sigma_1\sigma_2\sigma_3\sigma_4 = -1$) and B ($\sigma_1\sigma_2\sigma_3\sigma_4 = 1$) is 1.1863×10^{-3} which is in good agreement with the one obtained from Eq. (49) This indicates that our expansion converges rapidly enough to stop at fourth order in j when $j = 1/6$.

IV. SPIN WAVES AND GAPS DUE TO QUANTUM FLUCTUATIONS

In the previous section we showed that there are two inequivalent degenerate collinear spin structures with $\sigma_1\sigma_2\sigma_3\sigma_4 = \pm 1$ and that the quantum fluctuations remove this degeneracy and select the spin structure with $\sigma_1\sigma_2\sigma_3\sigma_4 = -1$ as the ground state. Here we will consider other quantities, such as spin waves and spin gaps, and the

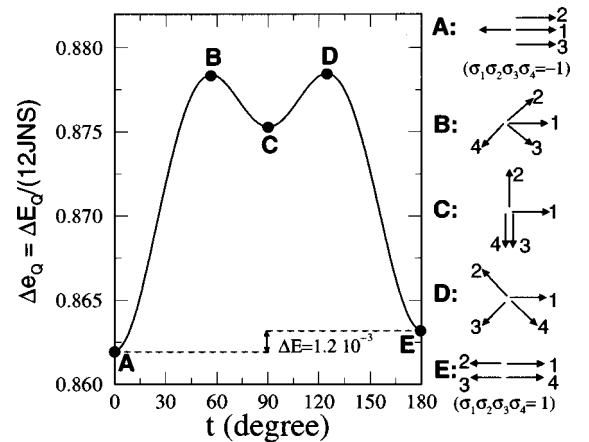


FIG. 3. Zero-point energy as a function of orientation of four antiferromagnetic sublattices for $J = J'$. If θ_α is the angle of sublattice α , the curve in the figure corresponds to the spin configurations where $\theta_1 = 0$, $\theta_2 = t$, $\theta_3 = -t$, and $\theta_4 = \pi + t$ where t varies from 0 to π . At the right side of the figure we show the particular spin configurations at points A, B, C, D, and E shown on the energy curve. Note that collinear configurations A and E have lower energy than noncollinear configurations. point A ($\sigma_1\sigma_2\sigma_3\sigma_4 = -1$) has slightly lower energy than Point E ($\sigma_1\sigma_2\sigma_3\sigma_4 = 1$) as shown analytically in the text.

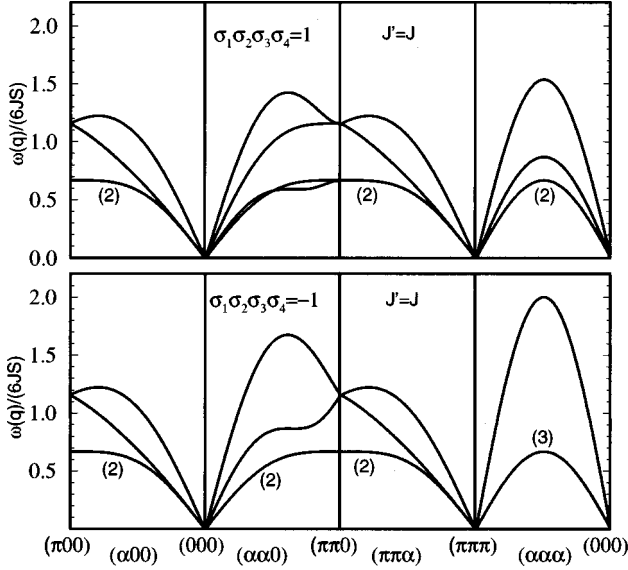


FIG. 4. Spin-wave spectrum (from noninteracting spin-wave theory) in the four-sublattice representation for two inequivalent collinear spin structures with $\sigma_1\sigma_2\sigma_3\sigma_4=1$ and $\sigma_1\sigma_2\sigma_3\sigma_4=-1$, respectively, for $J'=J$. The degeneracy of the modes (if more than one) is also shown in parenthesis.

temperature dependence of the sublattice magnetization for the ground-state structure, i.e., for $\sigma_1\sigma_2\sigma_3\sigma_4=-1$. Apart from being the ground state, the other nice thing about the spin configuration with $\sigma_1\sigma_2\sigma_3\sigma_4=-1$ is that the Hamiltonian matrices \mathbf{H}_1 and \mathbf{H}_2 (or matrices \mathbf{C} and \mathbf{S}) in Eqs. (31) commute ($[\mathbf{H}_1, \mathbf{H}_2]=0$) and thus we can diagonalize them simultaneously. This enables us to perform the diagonalization analytically at any \mathbf{q} point, as discussed in Appendix A, and obtain the spin-wave spectrum as

$$\omega_m^2(\mathbf{q}) = (6JS)^2 [1 + \gamma(\mathbf{q}) + 4j c_m(\mathbf{q})] \times [1 - \gamma(\mathbf{q}) + 4j s_m(\mathbf{q})] \quad m=1,2,3,4. \quad (56)$$

Here $c_m(\mathbf{q})$ and $s_m(\mathbf{q})$ are the eigenvalues of $\mathbf{C}(\mathbf{q})$ and $\mathbf{S}(\mathbf{q})$ matrices in Eqs. (24) and (25) which are given in Appendix A. In the absence of single-ion anisotropy, this result is equivalent to that obtained by Collins,²⁵ as we shall see below.

The spin-wave spectrum given above is compared with that of the other collinear structure with $\sigma_1\sigma_2\sigma_3\sigma_4=1$ in Fig. 4. From only the dispersion curves along principal directions it is not possible to tell which structure has the lower zero-point energy. However, our calculations show that the ground state is the one which has the lower symmetry. It is particularly important to note that the four spin-wave modes all have zero energy at $\mathbf{q}=0$ where $\gamma(\mathbf{q})=1$ and $s_m(\mathbf{q})=0$ and at $\mathbf{q}=(\pi/a)(1,1,1)$ where $\gamma(\mathbf{q})=-1$ and $c_m(\mathbf{q})=0$. This is exactly what one expects in the classical limit, i.e., $S \rightarrow \infty$ where the four antiferromagnetic sublattices are decoupled in the mean-field sense. However the absence of a spin-wave gap is a little surprising at first glance, as we included quantum fluctuations via linear spin-wave theory in our calculation, and it is these fluctuations which give rise to an effective interaction between the AF sublattices and force them to be collinear. Hence one would expect that including

the effect of quantum fluctuations should open a gap at the zone center, as pointed out in Ref. 3 and verified by experiment.¹⁷⁻¹⁹ Thus, even though linear spin-wave theory is able to predict an effective interaction due to zero-point motions of the spins, it is not capable of predicting the expected gap at $\mathbf{q}=0$. Here we use an approach alternate to that of Ref. 3, namely we use the Dyson-Maleev²⁰ transformation to treat spin-wave interactions correctly to leading order in $(1/S)$. In agreement with Ref. 3 we find that within linearized spin-wave theory the contribution to $\omega^2(\mathbf{q})$ from spin-wave interactions arises at relative order $J'^2/(J^2S)$ and is the same for both collinear structures. At higher orders in (J'/J) the quantum gap for the two different collinear spin structure will be different. However we do not expect this difference to be significant. Therefore we only consider the contributions to the spin gap at second order in (J'/J) . We will obtain this gap in two different approaches. First we will do this by introducing effective biquadratic interactions between sublattices to account for the effect of quantum fluctuations:

$$\Delta E_Q \sim -\frac{Q}{S^3} (\mathbf{S}_1 \cdot \mathbf{S}_2)^2. \quad (57)$$

This approach will be practically very useful to obtain the degeneracy and a qualitative estimate of the spin-wave gaps at $\mathbf{q}=0$. In the next subsection we will corroborate this approach by analyzing the effect of the four-operator terms in the boson Hamiltonian. At the end of this section, we will discuss the experimental consequences of the spin gap, its temperature dependence, etc.

In the remainder of this paper we will be concerned with the properties of the structure with $\sigma_1\sigma_2\sigma_3\sigma_4=-1$, i.e., the structure of the second kind, type A, shown in Fig. 2. Notice from Table II that this is the only structure for which θ_α is independent of α . Accordingly, for this structure, the coefficients in Eq. (12) depend only on $\mathbf{r}_j - \mathbf{r}_i$. Then it is appropriate to describe the structure with a unit cell whose basis vectors are

$$\mathbf{a}_1 = \frac{1}{2}a(\hat{i} + \hat{j}), \quad \mathbf{a}_2 = \frac{1}{2}a(\hat{i} + \hat{k}), \quad \mathbf{a}_3 = \frac{1}{2}a(\hat{j} + \hat{k}), \quad (58)$$

and the associated basis vectors for the reciprocal lattice are

$$\mathbf{b}_1 = (2\pi/a)(\hat{i} + \hat{j} - \hat{k}), \quad \mathbf{b}_2 = (2\pi/a)(\hat{i} - \hat{j} + \hat{k}), \quad \mathbf{b}_3 = (2\pi/a)(-\hat{i} + \hat{j} + \hat{k}). \quad (59)$$

The volume of the corresponding unit cell (BZ) is four times that of the sc BZ introduced above. As a result we now write

$$a_\alpha^+(i) = \frac{1}{\sqrt{4N}} \sum_{\mathbf{q} \in \text{BZ}} a_\alpha^+(\mathbf{q}) e^{i\mathbf{q} \cdot \mathbf{r}_i}, \quad (60)$$

where the sum over \mathbf{q} extends over the BZ defined by Eq. (59). In this representation H_1 and H_2 are scalars given by

$$H_1 = 6JS + 2J'S \{ \cos [a(q_x - q_y)/2] + \cos [a(q_x - q_z)/2] + \cos [a(q_z - q_y)/2] \} \\ H_2 = 6JS \gamma(\mathbf{q}) + 2J'S \{ \cos [a(q_x + q_y)/2] + \cos [a(q_x + q_z)/2] + \cos [a(q_z + q_y)/2] \}. \quad (61)$$

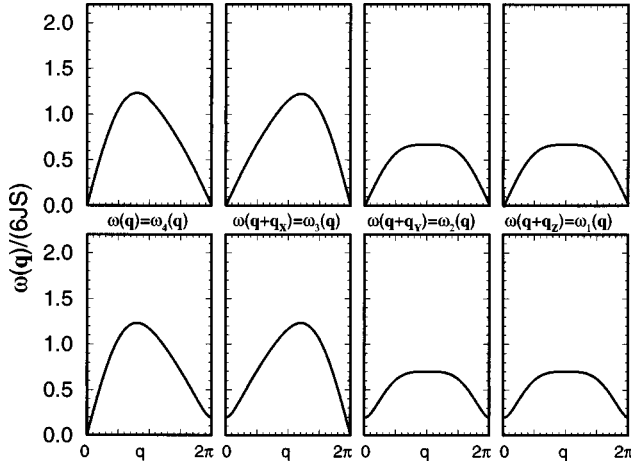


FIG. 5. Spin-wave spectrum of the collinear ground-state structure with $\sigma_1\sigma_2\sigma_3\sigma_4 = -1$ (antiferromagnet of the second kind, type A) in the one-sublattice representation, with (bottom panels) and without (top panels) spin-wave interactions. The top four panels [for $0 < q < \pi/a$ reproduce the entire spectrum of the four-sublattice representation on the line $(q,0,0)$]. The bottom panels show the effect of spin-wave interactions in opening a gap for all the non-Goldstone modes which had zero energy within linearized spin-wave theory. These results are evaluated for parameters appropriate to MnO: $S = 5/2$, $J/k_B = J'/k_B = 5$ K. Here $\mathbf{q} = (q,0,0)$ and \mathbf{q}_x , \mathbf{q}_y , and \mathbf{q}_z are defined in Eq. (61).

Thereby one finds a single mode whose energy is given by

$$\omega^2(\mathbf{q}) \equiv \omega_4^2(\mathbf{q}) = (6JS)^2 [1 + \gamma(\mathbf{q}) + 4jc_4(\mathbf{q})] \times [1 - \gamma(\mathbf{q}) + 4js_4(\mathbf{q})], \quad (62)$$

where c_4 and s_4 are given in Appendix A. The four branch spectrum of Eq. (56) is obtained by ‘‘folding over’’ the single branch spectrum of Eq. (62) so that modes at the four wave vectors,

$$\begin{aligned} \mathbf{q}_1 &= \mathbf{q}, & \mathbf{q}_2 &= \mathbf{q} + (2\pi/a)(1,0,0) = \mathbf{q} + \mathbf{q}_x, \\ \mathbf{q}_3 &= \mathbf{q} + (2\pi/a)(0,1,0) = \mathbf{q} + \mathbf{q}_y, & (63) \\ \mathbf{q}_4 &= \mathbf{q} + (2\pi/a)(0,0,1) = \mathbf{q} + \mathbf{q}_z \end{aligned}$$

are all associated with wave vector \mathbf{q} of the smaller sc BZ. In the representation of Eq. (62), these four wave vectors are inequivalent, modulo the reciprocal lattice of Eq. (59), whereas in the representation of Eq. (56), these wave vectors are equivalent. One can see that evaluating $c_4(\mathbf{q})$ and $s_4(\mathbf{q})$ at the four wave vectors of Eq. (63) yields the set of $c_m(\mathbf{q})$ and $s_m(\mathbf{q})$ for $m = 1,2,3,4$. The relation between the spectrum of Eq. (56) and that of Eq. (62) is illustrated by the comparison of Fig. 4 to the top set of panels of Fig. 5, where the spectrum of Eq. (62) is plotted for the wave vectors of Eq. (63).²⁶ The representation based on the BZ of Eq. (62) is useful because at any wave vector the inelastic neutron-scattering cross section is nonzero only for the single mode appearing in this basis. (Within the sc BZ basis, only one of the four modes is observable at any given wave vector.)

A. Effective biquadratic exchange interactions

Here we study the effect of biquadratic exchange interactions on the ground state and the spin-wave spectrum at zero wave vector. In the next section we will show that the effects of quantum fluctuations at lowest order in (J'/J) can be represented by an effective biquadratic interaction⁵ of the form

$$\Delta\mathcal{H}_Q^{\text{eff}} = -\frac{1}{2}Q \sum_{i,j} \Delta_{ij} [\mathbf{S}(i) \cdot \mathbf{S}(j)]^2 / S^3, \quad (64)$$

where Δ_{ij} is unity if spins i and j are nearest neighbors and is zero otherwise. In the next subsection we will analyze the effect of spin-wave interactions on the spin-wave spectrum at zero wave vector and by identifying those results with those from the effective interaction of Eq. (64), we will obtain an evaluation of Q in terms of the parameters J and J' of our model. As a result Q is of order $(J'/J)^2$. Note that this biquadratic interaction does not break the degeneracy between the collinear states but nevertheless can open a spin-wave gap at $\mathbf{q} \neq 0$. An advantage of this phenomenological biquadratic interaction is that it forms the basis of a renormalization-group discussion of properties near the critical point.²⁷

From Eq. (11), one obtains, after keeping only the quadratic interactions,

$$[\mathbf{S}(i) \cdot \mathbf{S}(j)]^2 / S^3 = S \cos^2 \theta_{j,i} + \frac{2}{S} \hat{O}_{j,i}^{(2)} \cos \theta_{j,i}, \quad (65)$$

where here and below the indices i, α are replaced, in the present single sublattice picture, by a single index i . Remembering that $\cos^2 \theta_{j,i} = 1$, and using Eq. (12), one can write

$$\begin{aligned} \Delta\mathcal{H}_Q^{\text{eff}} &= \text{const} + \sum_{i,j} \Delta_{ij} \left\{ Q [a^+(i)a(i) + a^+(j)a(j)] \right. \\ &\quad - \frac{Q}{2} [1 + \cos \theta_{j,i}] [a^+(i)a(j) + a(i)a^+(j)] \\ &\quad \left. + \frac{Q}{2} [1 - \cos \theta_{j,i}] [a^+(i)a^+(j) + a(i)a(j)] \right\}. \end{aligned} \quad (66)$$

This equation indicates that adding $\Delta\mathcal{H}_Q^{\text{eff}}$ to the Hamiltonian in Eq. (14) leads to

$$\begin{aligned} H_1 &= 6(JS + 2Q) + 2(J'S - Q) \{ \cos [a(q_x - q_y)/2] \\ &\quad + \cos [a(q_x - q_z)/2] + \cos [a(q_z - q_y)/2] \} \\ &= 6JS \left[\left(1 + \frac{2Q}{JS} \right) + \left(2j - \frac{Q}{3JS} \right) [c_4(\mathbf{q}) + s_4(\mathbf{q})] \right], \\ H_2 &= 6JS \gamma(\mathbf{q}) + 2(J'S + Q) \{ \cos [a(q_x + q_y)/2] \\ &\quad + \cos [a(q_x + q_z)/2] + \cos [a(q_z + q_y)/2] \} \\ &= 6JS \left[\gamma(\mathbf{q}) + \left(2j + \frac{Q}{3JS} \right) [c_4(\mathbf{q}) - s_4(\mathbf{q})] \right]. \end{aligned} \quad (67)$$

This leads to the energy spectrum

$$\omega(\mathbf{q})^2 = (6JS)^2 \left[1 + \gamma(\mathbf{q}) + \frac{2Q}{JS} \left(1 - \frac{s_4(\mathbf{q})}{3} \right) + \frac{2J'}{3J} c_4(\mathbf{q}) \right] \\ \times \left[1 - \gamma(\mathbf{q}) + \frac{2Q}{JS} \left(1 - \frac{c_4(\mathbf{q})}{3} \right) + \frac{2J'}{3J} s_4(\mathbf{q}) \right]. \quad (68)$$

In this representation, the true Goldstone modes occur when

$$\gamma(\mathbf{q}) = 1, \quad s_4(\mathbf{q}) = 0, \quad c_4(\mathbf{q}) = 3, \quad (69a)$$

or

$$\gamma(\mathbf{q}) = -1, \quad c_4(\mathbf{q}) = 0, \quad s_4(\mathbf{q}) = 3. \quad (69b)$$

If we write the wave vector in the form

$$\mathbf{q} = (2\pi/a)(H, K, L), \quad (70)$$

then the first case corresponds to H , K , and L either all even integers or all odd integers and the second case corresponds to $H - \frac{1}{2}$, $K - \frac{1}{2}$, $L - \frac{1}{2}$ either all even integers or all odd integers. The inelastic neutron-scattering cross section vanishes in the first case and is divergent in the second case (just as happens for a sc two-sublattice antiferromagnet). The modes which have fluctuation-induced gaps occur when

$$\gamma(\mathbf{q}) = 1, \quad s_4(\mathbf{q}) = 0, \quad c_4(\mathbf{q}) = -1, \quad (71a)$$

or

$$\gamma(\mathbf{q}) = -1, \quad c_4(\mathbf{q}) = 0, \quad s_4(\mathbf{q}) = -1, \quad (71b)$$

namely at wave vectors in each zone for which either one or two of H , K , and L are even integers and the rest are odd integers or when one or two of $H - \frac{1}{2}$, $K - \frac{1}{2}$, and $L - \frac{1}{2}$ are even integers and the rest are odd integers. As before, the neutron-scattering cross section is zero when $\gamma(\mathbf{q}) = 1$ and is large (divergent for $Q \rightarrow 0$) when $\gamma(\mathbf{q}) = -1$. As we discuss below, the spectrum shown in the bottom panels of Fig. 5 is essentially the spectrum one gets for the value of Q appropriate to describe fluctuations. At the three wave vectors of Eq. (71) one has a gap, induced by interactions, so that

$$\omega_0^2(\mathbf{q}) \approx (6JS)^2 \left[1 - \frac{1}{3} c_4(\mathbf{q}) \right] (2Q/JS) = 192JSQ. \quad (72)$$

Thus, when interactions are taken into account, only the true Goldstone modes have zero energy.

B. Interacting spin-wave theory—Hartree decoupling of fourth-order interaction terms

The objective of this section is to obtain spin-wave gaps by including the effect of quantum zero-point motion. In the previous subsection we showed that a biquadratic exchange interaction given in Eq. (64) leads to a nonzero spin-wave energy for all but the Goldstone modes. Here we perform an interacting spin-wave calculation using the standard Hartree decoupling of the fourth-order interaction terms which is known to give correctly all contributions to the spin-wave energies at relative order $(1/S)$. Since the procedure gives the same structure of the spin-wave spectrum at zero wave vector as does biquadratic exchange, we may use its result to determine an effective value for the biquadratic coupling constant, Q in Eq. (64). The result we will obtain is that

$$Q = -\frac{1}{2} J' \{ [\langle a^+(i)a^+(j) \rangle]_{\text{ap}} + [\langle a^+(i)a(j) \rangle]_{\text{p}} \} \\ = O((J')^2/J), \quad (73)$$

where $\langle \dots \rangle$ indicates a ground-state expectation value and the subscripts ‘‘p’’ and ‘‘ap’’ label nearest neighboring spins which are parallel and antiparallel, respectively.

For this calculation we use the Dyson-Maleev transformation given in Eqs. (7)–(9) and the local quantization axis defined by the rotation matrix in Eq. (6). Thus, one can obtain

$$\mathbf{S}(i) \cdot \mathbf{S}(j) = S^2 \cos \theta_{j,i} + \hat{O}_{j,i}^{(2)} + \hat{O}_{j,i}^{(4)} + O(1/S), \quad (74)$$

where $\hat{O}_{j,i}^{(2)}$ is obtained from Eq. (12) and the four operator term $\hat{O}_{j,i}^{(4)}$ is

$$\hat{O}_{j,i}^{(4)} = \frac{1}{4} [1 + \cos \theta_{j,i}] [2n(i)n(j) - a^+(i)a^+(i)a(i)a(j) \\ - a^+(j)a^+(j)a(j)a(i)] - \frac{1}{4} [1 - \cos \theta_{j,i}] [2n(i)n(j) \\ + a^+(i)a^+(i)a(i)a^+(j) + a^+(j)a^+(j)a(j)a^+(i)]. \quad (75)$$

In first order in $1/S$ we simply take out all nonzero contractions of operator averages, to get an effective biquadratic interaction from $\hat{O}_{j,i}^{(4)}$,

$$\hat{O}_{j,i}^{(4),\text{eff}} = \text{const} + \frac{1}{2} L [1 + \cos \theta_{j,i}] [a^+(i) - a^+(j)] \\ \times [a(i) - a(j)] - \frac{1}{2} M [1 - \cos \theta_{j,i}] [a^+(i) + a(j)] \\ \times [a^+(j) + a(i)] + V^{2,\text{eff}}, \quad (76)$$

where i and j are nearest neighboring sites,

$$L = \langle a^+(i)a(i) \rangle - [\langle a^+(i)a(j) \rangle]_{\text{p}}, \quad (77)$$

$$M = \langle a^+(i)a(i) \rangle + [\langle a^+(i)a^+(j) \rangle]_{\text{ap}},$$

and

$$V^{2,\text{eff}} = \frac{1}{2} \langle a^+(i)a(i) \rangle [1 - \cos \theta_{j,i}] [a(i)a(j) - a^+(i)a^+(j)]. \quad (78)$$

In order to get the above expressions, we used the fact that operator averages of the terms which have the factor $[1 + \cos \theta_{j,i}]$ only need to be taken over parallel spins. Similarly those terms which have the factor $[1 - \cos \theta_{j,i}]$ need to be averaged over antiparallel spins.

Inclusion of $\hat{O}_{j,i}^{2,\text{eff}}$ will enable us to include effects of spin-wave interactions correctly at first order in $1/S$. Corrections to the spin-wave spectrum at higher order in $1/S$ will be considered elsewhere.²⁸ Note that the anti-Hermitian term $V^{2,\text{eff}}$ only starts to contribute at second order in $1/S$. Accordingly, in what follows we will drop its contribution to $\hat{O}_{j,i}^{2,\text{eff}}$.

Then using the same argument given in the previous section, one can easily see that adding $\hat{O}_{j,i}^{(2),\text{eff}}$ into the Hamiltonian leads to the results

$$H_1(\mathbf{q}) = 6JS \left[\left(1 + \frac{J'(L-M)}{JS} \right) + \frac{J'}{3J} \left(1 - \frac{L}{S} \right) [c_4(\mathbf{q}) + s_4(\mathbf{q})] \right], \quad (79)$$

$$H_2(\mathbf{q}) = 6JS \left[\gamma(\mathbf{q}) + \frac{J'}{3J} \left(1 - \frac{M}{S} \right) [c_4(\mathbf{q}) - s_4(\mathbf{q})] \right]. \quad (80)$$

Therefore the spin-wave energy is now

$$\begin{aligned} \omega^2(\mathbf{q}) = & (6JS)^2 \left[1 + \gamma(\mathbf{q}) + \frac{2J'}{3J} c_4(\mathbf{q}) + \frac{J'(L-M)}{JS} \left[1 - \frac{1}{3} s_4(\mathbf{q}) \right] - \frac{J'}{JS} (L+M) c_4(\mathbf{q}) \right] \left[1 - \gamma(\mathbf{q}) + \frac{2J'}{3J} s_4(\mathbf{q}) \right. \\ & \left. + \frac{J'(L-M)}{JS} \left[1 - \frac{1}{3} c_4(\mathbf{q}) \right] - \frac{J'}{JS} (L+M) s_4(\mathbf{q}) \right]. \end{aligned} \quad (81)$$

We see that the Goldstone modes still occur when the condition of Eq. (69) is satisfied. The fluctuation-induced gaps at the wave vectors of Eq. (71) are given by

$$\omega_0^2 \approx (8/3)(6JS)^2 \frac{J'(L-M)}{JS} \approx -96JJ'S \{ [\langle a^+(i)a^+(j) \rangle]_{\text{ap}} + [\langle a^+(i)a(j) \rangle]_{\text{p}} \}. \quad (82)$$

Comparing this with Eq. (72) one identifies Q as in Eq. (73). Note that because Eqs. (68) and (81) are not of the same form, this identification of Q only applies to the zero wave vector spectrum. However, for the actual values of J', J, L , and M , the modified spin-wave spectra obtained from Eq. (81) and from the effective biquadratic interaction given in Eq. (68) (with Q from above equation) are almost identical over the whole zone because, as one sees in Fig. 5, quantum corrections to the spin-wave energy occur mainly at wave vectors close to those of Eq. (71), where they open a gap. The true Goldstone modes remain at zero energy, of course.

We now evaluate the spin gaps numerically. We start by evaluating

$$[\langle a^+(i)a(j) \rangle]_{\text{p}} = \langle a^+(i)a(j) \rangle_{j=i+\frac{1}{2}a(\hat{i}-\hat{j})} = \frac{1}{4N} \sum_{\mathbf{q} \in Z} [c_{xz}(\mathbf{q}) + s_{xz}(\mathbf{q})] \langle a^+(\mathbf{q})a(\mathbf{q}) \rangle, \quad (83)$$

where $\mathbf{q} \in Z$ indicates that the sum is over the Brillouin zone defined by Eq. (59) and $4N$ is the total number of spins in the system: $\sum_{\mathbf{q} \in Z} 1 = 4N$. Using the transformation to normal modes given in Appendix A, one obtains

$$\begin{aligned} [\langle a^+(i)a(j) \rangle]_{\text{p}} &= \frac{1}{4N} \sum_{\mathbf{q} \in Z} [c_{xz}(\mathbf{q}) + s_{xz}(\mathbf{q})] [m_{\mathbf{q}}^2 + (l_{\mathbf{q}}^2 + m_{\mathbf{q}}^2)n(T)] = \frac{1}{8N} \sum_{\mathbf{q} \in Z} [c_{xz}(\mathbf{q}) + s_{xz}(\mathbf{q})] \left[\frac{H_1(\mathbf{q}) - \omega(\mathbf{q})}{\omega(\mathbf{q})} + \frac{2H_1(\mathbf{q})}{\omega(\mathbf{q})} n(T) \right] \\ &= \frac{1}{8N} \sum_{\mathbf{q} \in Z} [c_{xz}(\mathbf{q}) + s_{xz}(\mathbf{q})] \frac{H_1(\mathbf{q})}{\omega(\mathbf{q})} [1 + 2n(T)], \end{aligned} \quad (84)$$

where

$$n(T) = 1/(e^{\omega/KT} - 1). \quad (85)$$

A similar evaluation yields

$$[\langle a^+(i)a^+(j) \rangle]_{\text{ap}} = -\frac{1}{8N} \sum_{\mathbf{q} \in Z} [c_{xz}(\mathbf{q}) - s_{xz}(\mathbf{q})] \frac{H_2(\mathbf{q})}{\omega(\mathbf{q})} [1 + 2n(T)]. \quad (86)$$

Hence, the spin-wave gap is

$$\begin{aligned} \omega_0^2 &= -96JJ'S \{ [\langle a^+(i)a^+(j) \rangle]_{\text{ap}} + [\langle a^+(i)a(j) \rangle]_{\text{p}} \} \\ &= -12JJ'S \frac{1}{N} \sum_{\mathbf{q} \in Z} \{ c_{xz}(\mathbf{q}) [H_1(\mathbf{q}) - H_2(\mathbf{q})] + s_{xz}(\mathbf{q}) [H_1(\mathbf{q}) + H_2(\mathbf{q})] \} \frac{1 + 2n(T)}{\omega(\mathbf{q})}. \end{aligned} \quad (87)$$

The details of the numerical evaluation of this expression at $T=0$ are discussed in Appendix B, where we obtain the result

$$\omega_0^2 = 4J'^2SY, \quad (88)$$

where Y is a dimensionless lattice sum, $Y \approx 1.366$.

One might think that the above procedure could be used to determine the temperature dependence of the gap. This approach would lead us to believe that the quantum gaps would *increase* as the temperature is increased. This behav-

ior strongly disagrees with experiments,^{18,19} which showed that the quantum gap has a temperature dependence close to that of the order parameter. In the boson calculation as outlined above, the result is that the quantum gap energy, ω_0 for a fixed value of J'/J is given by

$$\omega_0^2 = (J')^2 S f_1[kT/(JS)], \quad (89)$$

where df_1/dx is positive. More generally one would expect a result of the form

$$\omega_0^2 = (J'S)^2 \left\{ (1/S) f_1[kT/(JS)] + (1/S^2) f_2[kT/(JS)] + O(1/S^3) \right\}. \quad (90)$$

Presumably, the second term dominates at all but the very lowest temperatures. A possible mechanism for this is that the spectral weight functions in a bosonic formulation are usually replaced, in a more accurate calculation, by spectral weight functions associated with spin operators, which have an amplitude proportional to $\langle S_z \rangle$ rather than to unity. Replacement of $\langle a^+(i)a^+(j) \rangle_T$ by $\langle S_z \rangle_T \langle a^+(i)a^+(j) \rangle_T$ would lead to the experimental result. We are presently considering how to make this argument in detail.

We have calculated the gap at zero temperature for MnO [i.e., using $S=5/2$, $J'/k_B=J/k_B=5$ K (Refs. 14, 21 and 22)]. At $T=0$ K one obtains a gap of about 1.5 meV. This magnitude of the gap is quite consistent with what is seen in experiment,²⁵ although a detailed interpretation of the gaps requires taking into account the dipolar induced anisotropy in addition to the mechanism discussed here.^{25,29}

V. SPIN REDUCTION AND TEMPERATURE DEPENDENCE OF MAGNETIZATION

We now discuss the zero-point spin reduction and temperature dependence of the staggered magnetization. We start by considering the expectation value of the sublattice magnetization, $S^z(i)$. Of course, this expectation value is independent of i . Thus we write

$$\langle S^z(i) \rangle = S - \langle a^+(i)a(i) \rangle = S - \frac{1}{4N} \sum_{\mathbf{q} \in Z} \langle a^+(\mathbf{q})a(\mathbf{q}) \rangle. \quad (91)$$

Using the canonical transformation of Appendix A, one can show that

$$\langle S^z(i) \rangle = S - \Delta S - \Delta S(T), \quad (92)$$

where the spin reduction due to zero-point fluctuations is

$$\begin{aligned} \Delta S &= \frac{1}{4N} \sum_{\mathbf{q} \in Z} m_{\mathbf{q}}^2 = \frac{1}{8N} \sum_{\mathbf{q} \in Z} \frac{H_1(\mathbf{q}) - \omega(\mathbf{q})}{\omega(\mathbf{q})} \\ &= -\frac{1}{2} + \frac{1}{8N} \sum_{\mathbf{q} \in Z} \frac{H_1(\mathbf{q})}{\omega(\mathbf{q})}, \end{aligned} \quad (93)$$

and the temperature-dependent spin reduction is

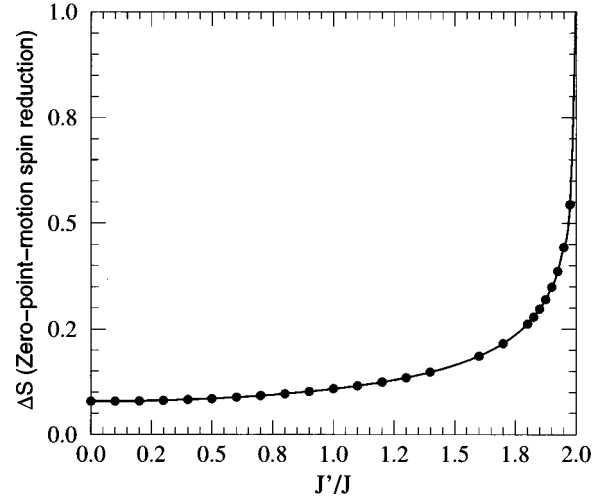


FIG. 6. Spin reduction due to quantum fluctuations as a function of the ratio J'/J . Each dot represents a numerical evaluation. Note that there is a divergence as $J'/J \rightarrow 2$ at which the classical system is not stable.

$$\begin{aligned} \Delta S(T) &= \frac{1}{4N} \sum_{\mathbf{q} \in Z} (l_{\mathbf{q}}^2 + m_{\mathbf{q}}^2) \langle \alpha(\mathbf{q})^+ \alpha(\mathbf{q}) \rangle \\ &= \frac{1}{4N} \sum_{\mathbf{q} \in Z} \frac{H_1(\mathbf{q})}{\omega(\mathbf{q})} \langle \alpha(\mathbf{q})^+ \alpha(\mathbf{q}) \rangle \\ &= \frac{1}{4N} \sum_{\mathbf{q} \in Z} \frac{H_1(\mathbf{q})}{\omega(\mathbf{q})} \frac{1}{e^{\omega(\mathbf{q})/kT} - 1}. \end{aligned} \quad (94)$$

Figure 6 shows the spin reduction due to zero-point fluctuations as a function of J'/J . At $J'=0$, we have four decoupled simple cubic antiferromagnetic sublattices and thus $\Delta S=0.078$, as calculated by Anderson.³⁰ Zero-point fluctuations increase slowly up to $J'/J=1$ and then very rapidly for $J'/J>1$ with a logarithmic divergence at $J'/J=2$. This behavior is very similar to that of the frustrated antiferromagnet on a square lattice.^{31,32} In fact, the transition expected here from the structure of the second kind, type A, to the structure of the third kind (see Fig. 2), is very similar to that between the (π, π) state and the $(\pi, 0)$ state investigated by Chubukov.^{31,32} It is interesting to note that as J'/J is increased, the system becomes unstable before $J'=2J$, where the classical model is unstable.

Our result for the zero-point spin reduction can be compared with similar results for other systems. For instance, Oguchi³³ calculated ΔS for an fcc lattice with a nearest-neighbor antiferromagnetic interaction and obtained the quite large value 0.33, an indication of very strong frustration. In our system, ΔS exceeds this value for $J'>1.85J$. Finally we note that at $T=0$ our calculation would say that we lose long-range order at $J'=1.964J$ for $S=1/2$, for instance.

The temperature dependence of the magnetization, $\Delta S(T)$, is shown in Fig. 7 for the parameters $S=5/2$, $J'/k_B=J/k_B=5$ K which are appropriate for MnO.¹⁴ It is interesting that T_N from our calculation comes very close to the experimental value. However, we expect this is coincidence as linear spin-wave theory usually reproduces the experimental magnetization at low T but underestimates the

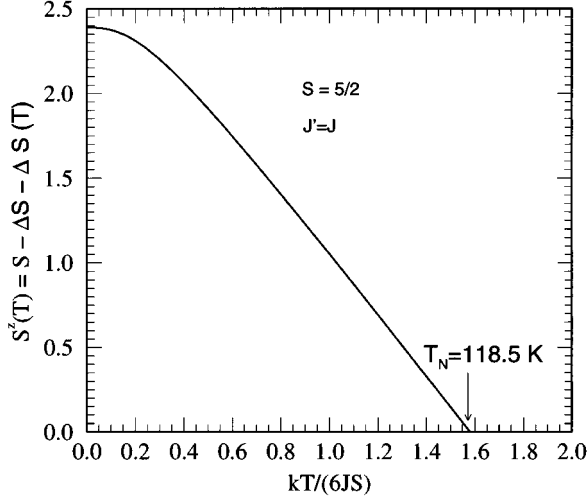


FIG. 7. Spin reduction due to both the zero-point and the thermal fluctuations. The plot is particularly for $S = 5/2$.

magnetization at temperature close to T_N . We also note that magnetization decreases linearly with increasing temperature. This is a surprising result as such a behavior was expected for a nearly 2D system.⁷

VI. DISCUSSION AND CONCLUSIONS

In summary we studied the quantum Heisenberg antiferromagnet on a face-centered-cubic lattice with first- and second-nearest-neighbor interactions J and J' , using interacting spin-wave theory with the standard Hartree decoupling approach. Our results can be summarized as follows:

(i) The infinite degeneracy of the ground-state manifold of this system is partially removed by collinear ordering in view of effects previously calculated by Shender at relative order $J'^2/(J^2S)$. Using symmetry arguments we showed that there are only two inequivalent collinear spin structures (i.e., $\sigma_1\sigma_2\sigma_3\sigma_4 = \pm 1$), which are degenerate at relative order $J'^2/(J^2S)$.

(ii) We then study the complete removal of the remaining degeneracy between these two inequivalent of collinear structures by analyzing the contribution to the spin-wave zero-point energy which is shown to be of the form;

$$\mathcal{H}_{\text{eff}}/J = C_0 + C_4\sigma_1\sigma_2\sigma_3\sigma_4(J'/J)^4 + O(J'/J)^5,$$

where C_4 , given in Eq. (55), is a positive constant. [The term of order $(J'/J)^5$ is also given explicitly.] Therefore the spin structure with $\sigma_1\sigma_2\sigma_3\sigma_4 = -1$, known as the *second kind of type A*, is chosen to be the ground state by quantum fluctuations. We note that in this particular spin configuration, the magnetic symmetry is trigonal and therefore the magnetic ordering should give rise to a structural distortion away from cubic symmetry. In fact, most of the monoxides of the iron group elements,^{14,21,22} such as MnO, have the magnetic structure found here and exhibit a small trigonal distortion from cubic symmetry. However we mention a caution that in these real systems there may be other energies, such as single-ion anisotropy, dipolar, or magnetoelastic interactions, which should be considered together with those discussed here.

(iii) In order to include the effect of quantum fluctuations on the spin-wave modes, we performed interacting spin-wave calculations using the standard Hartree decoupling of the fourth-order interaction terms. Quantum fluctuations are found to modify the spectrum of low-energy spin waves. In particular they cause the modes associated with the classical degeneracy to have nonzero energy. We showed that this gap and the modified spin-wave spectrum due to quantum fluctuations can be very well modeled by an effective biquadratic interactions of the form:

$$\Delta\mathcal{H}_Q^{\text{eff}} = -\frac{1}{2}Q\sum_{i,j}[\mathbf{S}(i)\cdot\mathbf{S}(j)]^2/S^3,$$

where Q is estimated to be

$$Q = -\frac{J'}{2}\{[\langle a^+(i)a^+(j) \rangle]_{\text{ap}} + [\langle a^+(i)a(j) \rangle]_{\text{p}}\} = O(J'^2/J),$$

where $\langle \dots \rangle$ indicates a ground-state expectation value.

(iv) We point out that the temperature dependence can be used to demonstrate whether or not the gap is due to quantum fluctuations.^{17,18} It is an open question to show definitively that this temperature dependence is nearly the same as that of the order parameter. We also show (in Appendix C) that the ratio of the high-temperature specific heat to the gap has a signature that can reveal whether or not the gap is due to quantum fluctuations.

(v) Finally we studied the spin reduction due to both quantum zero-point and thermal fluctuations. At $T = 0$ K, the zero-point spin reduction is quite large and strongly depends on the ratio of J'/J . When this ratio approaches 2, where the *second kind* magnetic spin structure is not stable classically, the zero-point fluctuations are very large and eventually destroy the long-range order in a manner similar to that found for the frustrated antiferromagnet on a square lattice.^{31,32} We also evaluate the temperature dependence of the sublattice magnetization. For the realistic values of parameters ($S = 5/2, J'/k_B = J/k_B = 5$ K) for MnO, we obtained $T_N = 118.5$ K, very close to the experimental value of 120 K.

ACKNOWLEDGMENTS

The work at the University of Pennsylvania was supported in part by the National Science Foundation under Grant No. 95-20175. A.B.H. acknowledges partial support from the EPSRC (UK) and the USIEF (Israel). He also thanks the Department of Theoretical Physics, Oxford University and the School of Physics and Astronomy, Tel Aviv University, for their hospitality during the final phases of this work.

APPENDIX A: DIAGONALIZATION OF THE QUADRATIC SPIN HAMILTONIAN

In this appendix, we discuss the diagonalization of the bosonic Hamiltonian in Eq. (14). We start from the Hamiltonian written as quadratic form of spin operators

$$\mathcal{H} = \frac{1}{2}\sum_{\mathbf{q}} \mathbf{X}^+(\mathbf{q})\mathbf{M}(\mathbf{q})\mathbf{X}(\mathbf{q}), \quad (\text{A1})$$

where $\mathbf{X}^+(\mathbf{q}) = [a_1(\mathbf{q}), \dots, a_n(\mathbf{q}), a_1^+(-\mathbf{q}), \dots, a_n^+(-\mathbf{q})]$ and for a hermitian \mathcal{H} , \mathbf{M} is

$$\mathbf{M}(\mathbf{q}) = \begin{pmatrix} \mathbf{H}_1(\mathbf{q}) & \mathbf{H}_2(\mathbf{q}) \\ \mathbf{H}_2(\mathbf{q}) & \mathbf{H}_1(\mathbf{q}) \end{pmatrix}. \quad (\text{A2})$$

Here we will treat only the case where $\mathbf{H}_1(\mathbf{q})$ and $\mathbf{H}_2(\mathbf{q})$ are real symmetric. In particular, we will obtain analytical expressions for eigenvalues and canonical transformation for the collinear ground state ($\sigma_1\sigma_2\sigma_3\sigma_4 = -1$) for which $[\mathbf{H}_1(\mathbf{q}), \mathbf{H}_2(\mathbf{q})] = 0$. A formal discussion of this problem with its most general form [where $\mathbf{H}_1(\mathbf{q})$ is Hermitian and $\mathbf{H}_2(\mathbf{q})$ is complex but symmetric] can be found in Ref. 34.

The diagonalization of the Hamiltonian in Eq. (A1) requires finding a canonical transformation $\mathbf{S}(\mathbf{q})$ defining quasiparticle operators

$$\mathbf{X}(\mathbf{q}) = \mathbf{S}(\mathbf{q})\mathbf{Y}(\mathbf{q}), \quad (\text{A3})$$

where $\mathbf{Y}^+(\mathbf{q}) = [\alpha_1(\mathbf{q}), \dots, \alpha_n(\mathbf{q}), \alpha_1^+(-\mathbf{q}), \dots, \alpha_n^+(-\mathbf{q})]$ and

$$\mathbf{S}(\mathbf{q}) = \begin{pmatrix} \mathbf{P} & \mathbf{Q} \\ \mathbf{Q} & \mathbf{P} \end{pmatrix} \quad \text{and} \quad \mathbf{S}^{-1}(\mathbf{q}) = \begin{pmatrix} \tilde{\mathbf{P}} & -\tilde{\mathbf{Q}} \\ -\tilde{\mathbf{Q}} & \tilde{\mathbf{P}} \end{pmatrix}. \quad (\text{A4})$$

It is easy to show that commutation relations yield

$$(\tilde{\mathbf{P}} - \tilde{\mathbf{Q}})(\mathbf{P} + \mathbf{Q}) = \mathbf{I} \quad \text{and} \quad \tilde{\mathbf{P}}\mathbf{Q} - \tilde{\mathbf{Q}}\mathbf{P} = \mathbf{0}, \quad (\text{A5})$$

and that the diagonalization condition, $[\alpha_n(\mathbf{q}), \mathcal{H}] = \omega_n(\mathbf{q})\alpha_n(\mathbf{q})$, yields

$$\mathbf{H}_1\mathbf{P} + \mathbf{H}_2\mathbf{Q} = \mathbf{P}\mathbf{\Omega} \quad \text{and} \quad \mathbf{H}_1\mathbf{Q} + \mathbf{H}_2\mathbf{P} = -\mathbf{Q}\mathbf{\Omega}, \quad (\text{A6})$$

where $\mathbf{\Omega}$ is a diagonal matrix with $\Omega_{ii} = \omega_i(\mathbf{q})$ $i = 1, \dots, n$. Adding and subtracting these equations give

$$(\mathbf{H}_1 + \mathbf{H}_2)(\mathbf{P} + \mathbf{Q}) = (\mathbf{P} - \mathbf{Q})\mathbf{\Omega}$$

and

$$(\mathbf{H}_1 - \mathbf{H}_2)(\mathbf{P} - \mathbf{Q}) = (\mathbf{P} + \mathbf{Q})\mathbf{\Omega}. \quad (\text{A7})$$

Thus combining these yields

$$\mathbf{D}(\mathbf{P} + \mathbf{Q}) \equiv (\mathbf{H}_1 - \mathbf{H}_2)(\mathbf{H}_1 + \mathbf{H}_2)(\mathbf{P} + \mathbf{Q}) = (\mathbf{P} + \mathbf{Q})\mathbf{\Omega}^2, \quad (\text{A8})$$

$$\tilde{\mathbf{D}}(\mathbf{P} - \mathbf{Q}) = (\mathbf{H}_1 + \mathbf{H}_2)(\mathbf{H}_1 - \mathbf{H}_2)(\mathbf{P} - \mathbf{Q}) = (\mathbf{P} - \mathbf{Q})\mathbf{\Omega}^2.$$

Thus the spin-wave energies $\omega(\mathbf{q})$ are found as the square

APPENDIX B: NUMERICAL EVALUATION OF THE GAP

Here we discuss the evaluation of Eq. (87) for the quantum gap. For simplicity we work in the limit $J'/(6J) \ll 1$, so that we have

$$\begin{aligned} \omega_0^2 &= -12JJ'S \frac{1}{N_{\mathbf{q} \in Z}} \sum_{\mathbf{q} \in Z} 2c_{xz}(\mathbf{q}) \left[\frac{H_1(\mathbf{q}) - H_2(\mathbf{q})}{H_1(\mathbf{q}) + H_2(\mathbf{q})} \right]^{1/2} \\ &= -24JJ'S \frac{1}{N_{\mathbf{q} \in Z}} \sum_{\mathbf{q} \in Z} c_{xz}(\mathbf{q}) \left[\frac{1 - \gamma(\mathbf{q}) + (2J'/3J)s_4(\mathbf{q})}{1 + \gamma(\mathbf{q}) + (2J'/3J)c_4(\mathbf{q})} \right]^{1/2} \\ &\approx -24JJ'S \frac{1}{N_{\mathbf{q} \in Z}} \sum_{\mathbf{q} \in Z} c_{xz}(\mathbf{q}) \left[\frac{1 - \gamma(\mathbf{q})}{1 + \gamma(\mathbf{q})} \right]^{1/2} \left[1 + \frac{J's_4(\mathbf{q})}{3J[1 - \gamma(\mathbf{q})]} - \frac{J'c_4(\mathbf{q})}{3J[1 + \gamma(\mathbf{q})]} \right] \\ &= 8J'^2S \frac{1}{N_{\mathbf{q} \in Z}} \sum_{\mathbf{q} \in Z} c_{xz}(\mathbf{q})^2 \frac{[1 - \gamma(\mathbf{q})]^{1/2}}{[1 + \gamma(\mathbf{q})]^{3/2}} \\ &\equiv 4J'^2SY, \end{aligned} \quad (\text{B1})$$

roots of the eigenvalues of $\mathbf{D}(\mathbf{q})$. We now concentrate on $\mathbf{M}(\mathbf{q})$ in Eq. (30) for the structure of the second kind, type A, shown in Fig. 2, for which $\sigma_1\sigma_2\sigma_3\sigma_4 = -1$ (say $\sigma_2 = \sigma_3 = \sigma_4 = -\sigma_1 = 1$). For this particular case, it is easy to see that $[\mathbf{H}_1, \mathbf{H}_2] = 0$ and thus \mathbf{H}_1 and \mathbf{H}_2 are simultaneously diagonalizable. Hence, the eigenvalues (spin modes) of \mathbf{D} in Eq. (34) are

$$\omega_m^2(\mathbf{q}) = (6JS)^2 [1 + \gamma(\mathbf{q}) + 4jc_m(\mathbf{q})] \times [1 - \gamma(\mathbf{q}) + 4js_m(\mathbf{q})] \quad m = 1, 2, 3, 4. \quad (\text{A9})$$

Here $c_m(\mathbf{q})$ and $s_m(\mathbf{q})$ are the eigenvalues of $\mathbf{C}(\mathbf{q})$ and $\mathbf{S}(\mathbf{q})$ matrices in Eqs. (24) and (25);

$$c_m(\mathbf{q}) = \begin{cases} c_{xy}(\mathbf{q}) & -c_{xz}(\mathbf{q}) - c_{yz}(\mathbf{q}) & \text{if } m=1, \\ -c_{xy}(\mathbf{q}) & +c_{xz}(\mathbf{q}) - c_{yz}(\mathbf{q}) & \text{if } m=2, \\ -c_{xy}(\mathbf{q}) & -c_{xz}(\mathbf{q}) + c_{yz}(\mathbf{q}) & \text{if } m=3, \\ c_{xy}(\mathbf{q}) & +c_{xz}(\mathbf{q}) + c_{yz}(\mathbf{q}) & \text{if } m=4, \end{cases}$$

$$s_m(\mathbf{q}) = \begin{cases} s_{xy}(\mathbf{q}) & -s_{xz}(\mathbf{q}) - s_{yz}(\mathbf{q}) & \text{if } m=1, \\ -s_{xy}(\mathbf{q}) & +s_{xz}(\mathbf{q}) - s_{yz}(\mathbf{q}) & \text{if } m=2, \\ -s_{xy}(\mathbf{q}) & -s_{xz}(\mathbf{q}) + s_{yz}(\mathbf{q}) & \text{if } m=3, \\ s_{xy}(\mathbf{q}) & +s_{xz}(\mathbf{q}) + s_{yz}(\mathbf{q}) & \text{if } m=4. \end{cases} \quad (\text{A10})$$

In the one sublattice approach, as discussed in the text, H_1 and H_2 are scalars and therefore we have

$$a(\mathbf{q}) = l_{\mathbf{q}}\alpha(\mathbf{q}) + m_{\mathbf{q}}\alpha(-\mathbf{q})^+, \quad (\text{A11})$$

where

$$l_{\mathbf{q}}^2 = \frac{H_1(\mathbf{q}) + \omega(\mathbf{q})}{2\omega(\mathbf{q})}, \quad m_{\mathbf{q}}^2 = \frac{H_1(\mathbf{q}) - \omega(\mathbf{q})}{2\omega(\mathbf{q})},$$

$$l_{\mathbf{q}}m_{\mathbf{q}} = -\frac{H_2(\mathbf{q})}{2\omega(\mathbf{q})}. \quad (\text{A12})$$

where

$$Y = \frac{2}{N} \sum_{\mathbf{q} \in Z} c_{xz}^2(\mathbf{q}) \frac{[1 - \gamma(\mathbf{q})]^{1/2}}{[1 + \gamma(\mathbf{q})]^{3/2}}. \quad (\text{B2})$$

In the above we used the fact that $\sum_{\mathbf{q} \in Z} c_{xz}(\mathbf{q}) f(\mathbf{q}) = 0$, when f is an orthogonal trigonometric function. Numerically we find $Y = 1.365\,94$, which, for MnO, leads to $\omega_0 = 1.5$ meV.

APPENDIX C: THE HIGH-TEMPERATURE SPECIFIC HEAT AND THE GAP

In this appendix we show that a measurement of the high-temperature specific heat can be used to distinguish whether the gap in the spin-wave spectrum is due to biquadratic exchange interactions or to quantum zero-point fluctuations. To this end we will calculate the high-temperature limiting value of CkT^2 , where C is the magnetic specific heat per spin. (We assume that experimental data can be analyzed to eliminate contributions from the lattice or nuclear spin degrees of freedom.)

We start from the standard formula³⁵ for the limiting value of the high-temperature specific heat per spin C from the Hamiltonian \mathcal{H} :

$$CkT^2 = N_s^{-1} [\text{Tr} \mathcal{H}^2 / (\text{Tr} 1) - (\text{Tr} \mathcal{H} / \text{Tr} 1)^2], \quad (\text{C1})$$

where N_s is the number of spins. We assume a Hamiltonian of the form

$$\mathcal{H} = \sum_{i < j} \mathcal{H}_{ij} \equiv \sum_{i < j} [J_{ij} \mathbf{S}_i \cdot \mathbf{S}_j + K_{ij} ([\mathbf{S}_i \cdot \mathbf{S}_j]^2 - C_0)], \quad (\text{C2})$$

where J scales the usual exchange interactions, K scales the biquadratic exchange interactions, and $C_0 = S^2(S+1)^2/3 \equiv X^2/3$ is a constant introduced to make the Hamiltonian traceless. We will entertain two scenarios: in the first $K_{ij} = 0$ so that the gap ω_0 is due entirely to quantum fluctuations. In the second, we attribute ω_0 to biquadratic exchange, in which case we set $J' = 0$. Our aim is to see how CkT^2 differs in these two limiting scenarios.

Equation (C1) yields

$$CkT^2 = \frac{1}{2} \sum_j \text{Tr} \mathcal{H}_{ij}^2 / Z_0, \quad (\text{C3})$$

where $Z_0 = \text{Tr} 1$. Take site i to be in sublattice 1, as in Fig. 1. Then the sum over j will be carried over six values of Δ_1 for which $J_{ij} = J$ and $K_{ij} = 0$ and over 12 values of the δ 's for which $J_{ij} = J'$ and $K_{ij} = Q/S^3$. Thus

$$CkT^2 = 3J^2 G_2 + 6(Q^2/S^6) [G_4 - 2C_0 G_2 + C_0^2] + 12(Q/S^3) J' G_3 + 6J'^2 G^2, \quad (\text{C4})$$

where $G_n = \text{Tr}(\mathbf{S}_i \cdot \mathbf{S}_j)^n / (\text{Tr} 1)$, with

$$G_2 = \frac{1}{3} X^2, \quad G_3 = -\frac{1}{6} X^2, \quad G_4 = \frac{1}{5} X^4 - \frac{2}{15} X^3 + \frac{2}{15} X^2. \quad (\text{C5})$$

We will now show that the value of $R \equiv CkT^2 / (J^2 X^2)$ assumes quite different values depending on whether the gap is due to quantum fluctuations or to biquadratic exchange. First of all, when the gap is due to Q and we set $J' = 0$, then

$$CkT^2 = J^2 X^2 + \frac{2Q^2}{15S^6} [4X^4 - 6X^3 + 6X^2]. \quad (\text{C6})$$

Also, when $J' = 0$, the gap at zero temperature ω_0 obeys

$$Q = \omega_0^2 / (192JS), \quad (\text{C7})$$

so that

$$CkT^2 = J^2 X^2 + \frac{2\omega_0^4}{15(192JS^4)^2} [4X^4 - 6X^3 + 6X^2], \quad (\text{C8})$$

and approximately (for large S),

$$R = 1 + \frac{24}{5} \left(\frac{\omega_0}{24JS} \right)^4. \quad (\text{C9})$$

When $Q = 0$, but J' is nonzero, then

$$CkT^2 = J^2 X^2 + 2J'^2 X^2 \quad (\text{C10})$$

and

$$\omega_0 = 2J' \sqrt{SY}, \quad (\text{C11})$$

where the constant Y , which is of order unity, is given in Appendix B. Thus

$$CkT^2 = \left(J^2 + \frac{\omega_0^2}{2SY} \right) X^2 \quad (\text{C12})$$

and (for large S)

$$R = 1 + \frac{\omega_0^2}{2SYJ^2}. \quad (\text{C13})$$

Numerical evaluation of these results in typical cases shows that R is very close to unity when $J' = 0$ (i.e., when the gap is due to biquadratic exchange) and is about 3 for parameters given below Eq. (87) appropriate to MnO. Thus measurement of the high-temperature magnetic specific heat can also be used to distinguish a gap due to biquadratic exchange from one due to quantum fluctuations.

- ¹For a review, see E. F. Shender and P. C. W. Holdsworth, in *Fluctuations and Order: The New Synthesis*, edited by M. Milonas (Springer-Verlag, Berlin, 1995).
- ²P. Chandra, P. Coleman, and A. I. Larkin, *Phys. Rev. Lett.* **64**, 88 (1989).
- ³E. F. Shender, *Sov. Phys. JETP* **56**, 178 (1982).
- ⁴Fluctuations cannot remove the degeneracy associated with a true symmetry of the system, such as an overall rotation of all spins in the examples we consider. In such cases, the ground state is “selected” only by the mechanism of “broken” symmetry in which an infinitesimal field is applied to the order parameter.
- ⁵C. L. Henley, *J. Appl. Phys.* **61**, 3962 (1987).
- ⁶K. Kubo and T. Kishi, *J. Phys. Soc. Jpn.* **60**, 567 (1990).
- ⁷E. Rastelli, S. Sedazzari, and A. Tassi, *J. Phys.: Condens. Matter* **2**, 8935 (1990).
- ⁸A. B. Harris, C. Kallin, and A. J. Berlinsky, *Phys. Rev. B* **45**, 2899 (1992).
- ⁹J.T. Chalker, P. C. W. Holdsworth, and E. F. Shender, *Phys. Rev. Lett.* **68**, 855 (1992).
- ¹⁰T. Yildirim, A. B. Harris, and E. F. Shender, *Phys. Rev. B* **53**, 6455 (1996).
- ¹¹J. Villain, R. Bidaux, J. P. Carton, and R. Conte, *J. Phys. (Paris)* **41**, 1263 (1980).
- ¹²C. L. Henley, *Phys. Rev. Lett.* **62**, 2056 (1989).
- ¹³E. F. Shender, V. B. Cherepanov, P. C. W. Holdsworth, and A. J. Berlinsky, *Phys. Rev. Lett.* **70**, 3812 (1993).
- ¹⁴Y. Yamamoto and T. Nagamiya, *J. Phys. Soc. Jpn.* **32**, 1248 (1971).
- ¹⁵*Encyclopedia of Physics*, edited by S. Flugge and H. P. J. Wijn, Vol. XVIII/2 (Ferromagnetism) (Springer-Verlag, Berlin, 1966).
- ¹⁶P. M. Chaikin and T. C. Lubensky, *Principles of Condensed Matter Physics* (Cambridge University Press, Cambridge, 1995), p. 432.
- ¹⁷A. Gukasov, Th. Bruckel, B. Dorner, V. P. Plakhty, W. Prandtl, E. F. Shender, and O. P. Smirnov, *Europhys. Lett.* **7**, 83 (1988).
- ¹⁸Th. Bruckel, B. Dorner, A. Gukasov, and V. Plakhty, *Phys. Lett. A* **162**, 357 (1992).
- ¹⁹M. Greven, Y.-J. Kim, R. J. Birgeneau, F.C. Chou, M. A. Kastner, D. S. Kleinberg, Y. S. Lee, G. Shirane, A. Aharony, O. Entin-Wohlman, and A. B. Harris (unpublished).
- ²⁰F. J. Dyson, *Phys. Rev.* **102**, 1217 (1956); S. V. Maleev, *Zh. Éksp. Teor. Fiz.* **33**, 1010 (1958) [*Sov. Phys. JETP* **6**, 778 (1958)].
- ²¹W. L. Roth, *Phys. Rev.* **110**, 1338 (1958).
- ²²C. G. Shull, W. A. Strauser, and E. O. Wollan, *Phys. Rev.* **83**, 133 (1951).
- ²³M. W. Long, *J. Phys.: Condens. Matter* **1**, 2857 (1989).
- ²⁴A. B. Harris, in *Disorder in Condensed Matter Physics*, edited by J. A. Blackman and J. Taguena (Clarendon, Oxford, 1991).
- ²⁵M. F. Collins, *Proceedings of the International Conference on Magnetism, Nottingham* (Institute of Physics, London, 1965).
- ²⁶One can show that the frequency-dependent susceptibility at wave vector \mathbf{q} involves the modes given by Eq. (62) for wave vectors \mathbf{q} and $\mathbf{q}+(1,1,1)\pi/a$. For the isotropic exchange model of the present paper, these two modes are degenerate, in which case the dispersion relation of the single sublattice would coincide exactly with that observed by inelastic neutron scattering. The fact that those experiments (Ref. 25) observe two modes at each wave vector indicates the presence of anisotropic interactions not considered here. One should also note that the gaps introduced by spin-wave interactions occur at reduced wave vector $\mathbf{q}=0$ in the four-sublattice representation, but at the nonzero values of \mathbf{q} given in Eq. (71) in the single sublattice picture. These gaps should therefore be observed in neutron scattering at the wave vectors of Eq. (71) and *not* at $\mathbf{q}=0$.
- ²⁷A. Aharony and A. B. Harris (unpublished).
- ²⁸N. Mohr and A. B. Harris (unpublished).
- ²⁹J. I. Kaplan, *J. Chem. Phys.* **22**, 1709 (1954).
- ³⁰P. W. Anderson, *Phys. Rev.* **86**, 694 (1952).
- ³¹F. Mila, D. Poilblanc, and C. Bruder, *Phys. Rev. B* **43**, 7891 (1991).
- ³²A. Chubukov, *Phys. Rev. B* **44**, 392 (1991).
- ³³T. Oguchi, H. Nishimori, and Y. Taguchi, *J. Phys. Soc. Jpn.* **54**, 4494 (1985).
- ³⁴J. P. Blaizot and G. Ripka, *Quantum Theory and Finite Systems* (The MIT Press, Cambridge, Massachusetts, 1986).
- ³⁵R. K. Pathria, *Statistical Mechanics* (Pergamon, Oxford, 1972), p. 91.